

Marquette University

e-Publications@Marquette

Dissertations (1934 -)

Dissertations, Theses, and Professional
Projects

Experimental & Simulation Approaches to Study Neuromuscular Control in People with Chronic Ankle Instability

Hoon Kim
Marquette University

Follow this and additional works at: https://epublications.marquette.edu/dissertations_mu



Part of the [Physical Therapy Commons](#)

Recommended Citation

Kim, Hoon, "Experimental & Simulation Approaches to Study Neuromuscular Control in People with Chronic Ankle Instability" (2020). *Dissertations (1934 -)*. 1030.
https://epublications.marquette.edu/dissertations_mu/1030

EXPERIMENTAL & SIMULATION APPROACHES TO STUDY
NEUROMUSCULAR CONTROL IN PEOPLE WITH CHRONIC ANKLE
INSTABILITY

by
Hoon Kim, M.A., A.T.C.

A Dissertation submitted to the Faculty of the Graduate School,
Marquette University,
in Partial Fulfillment of the Requirements for
the Degree of Doctor of Philosophy

Milwaukee, Wisconsin

December 2020

ABSTRACT
EXPERIMENTAL & SIMULATION APPROACHES TO STUDY
NEUROMUSCULAR CONTROL IN PEOPLE WITH CHRONIC ANKLE
INSTABILITY

Hoon Kim, M.A., A.T.C.

Marquette University, 2020

Ankle sprains are among the most common musculoskeletal injuries, and up to 70% of people who sprain their ankles develop chronic ankle instability (CAI). Moreover, people who develop CAI have a significantly higher risk of developing ankle osteoarthritis. Recent research has identified neuromuscular deficits that may be responsible for the high recurrence rates of ankle sprains and for the progression towards ankle osteoarthritis in people with CAI. Unfortunately, current rehabilitation strategies are not completely successful because the mechanisms responsible for these deficits are not fully elucidated. Therefore, the purpose of this dissertation was to investigate individual muscle forces and force generating capacities, the contributions of individual muscles to ankle joint contact forces, muscle activation patterns in the time-frequency domain, and central nervous system control strategies in people with CAI.

Eleven people with CAI and 11 matched healthy control performed landing, anticipated cutting, and unanticipated cutting tasks, while three-dimensional movement, ground reaction force, and muscle activation data were collected with motion capture system, force plate, and electromyography, respectively. In the first study, a musculoskeletal model and static optimization were used to estimate the force and force generating capacity of individual muscles. In the second study, an additional joint reaction analysis was used in combination with the musculoskeletal model to estimate the contribution of individual muscle forces to ankle joint contact forces. In the third study, wavelet transformation and principal component analysis were used to analyze the time-frequency domain of muscle activation patterns. In the final study, non-negative matrix factorization was used to extract muscle synergies in order to identify central nervous system control strategies. Results from all analyses were compared between people with and without CAI.

The primary findings of this dissertation were that, compared to healthy controls, people with CAI exhibit 1) greater muscle forces and/or force generating capacities in proximal muscles, 2) greater ankle anterior shear forces during early and late stance phases of unanticipated cutting, 3) lower intensity of muscle activation and a task-dependent inability to shift activation towards higher frequencies, and 4) similar complexity in neuromuscular control from a central nervous system perspective.

ACKNOWLEDGMENTS

Hoon Kim, M.A., A.T.C.

I would like to thank people who have assisted and supported me. First, I would like to thank my committee members. Drs. Kristof Kipp, Andrew Starsky, and Karen Kruger have provided valuable guidance, expertise, and countless hours in assisting in the completion of my dissertation. Their help has been instrumental in my success at Marquette University and finishing my Ph.D. project.

I would especially like to thank Dr. Kristof Kipp who is my major professor, advisor, and mentor. His guidance and support have been crucial in achieving my goals. I am grateful for having the opportunity to study and learn from his mentoring throughout my doctoral training.

I would like to thank the current and past members (Philip Malloy, John Krzyszkowski, Alec Miller, William Wolf, Marwan Aljohani, Christopher Geiser, Nayun Ahn, Michael Haischer, Gretchen Geiser) of the biomechanics laboratory for their scientific support and friendship.

I would also like to thank my wife Ahhee Cho for her unconditional love, patience, and support throughout this entire process. Without her, I would have never been able to achieve this.

TABLE OF CONTENTS

ACKNOWLEDGMENTS	i
LIST OF TABLES	iv
LIST OF FIGURES	v
CHAPTER 1: INTRODUCTION	1
CHAPTER 2: PEAK FORCES AND FORCE GENERATING CAPACITIES OF LOWER EXTREMITY MUSCLES DURING DYNAMIC TASKS IN PEOPLE WITH AND WITHOUT CHRONIC ANKLE INSTABILITY	7
INTRODUCTION	7
METHODS	10
RESULTS	15
DISCUSSION	20
CONCLUSION	24
CHAPTER 3: MUSCLE FORCE CONTRIBUTIONS TO ANKLE JOINT CONTACT FORCES DURING AN UNANTICIPATED CUTTING TASK IN PEOPLE WITH CHRONIC ANKLE INSTABILITY	25
INTRODUCTION	25
METHODS	27
RESULTS	32
DISCUSSION	37
CONCLUSION	41
CHAPTER 4: TIME-FREQUENCY ANALYSIS OF MUSCLE ACTIVATION PATTERNS IN PEOPLE WITH CHRONIC ANKLE INSTABILITY DURING LANDING AND CUTTING TASKS	42
INTRODUCTION	42
METHODS	44
RESULTS	49

DISCUSSION.....	52
CONCLUSION.....	57
CHAPTER 5: MUSCLE SYNERGIES IN PEOPLE WITH CHRONIC ANKLE INSTABILITY DURING ANTICIPATED AND UNANTICIPATED CUTTING TASKS	58
INTRODUCTION	58
METHODS	60
RESULTS	64
DISCUSSION.....	68
CONCLUSION.....	71
CHAPTER 6: CONCLUSION	73
BIBLIOGRAPHY.....	80

LIST OF TABLES

CHAPTER 2

Table 2. 1 Demographic information. (CAI: chronic ankle instability group, CON: control group, FADI: Foot & Ankle Disability Index, FADIS: Foot & Ankle Disability Index in Sports, Tegner: Tegner's score)..... 10

Table 2. 2 Mean and standard deviation of muscle force. (CAI: chronic ankle instability group, CON: control group, LAND: landing, ANT: anticipated cutting, UNANT: unanticipated cutting, SL: soleus, MG, medial gastrocnemius, LG: lateral gastrocnemius, TA: tibialis anterior, FL: fibularis longus, VAS: vastus muscles, RF: rectus femoris, GX: gluteus maximus, GM: gluteus medius, HAMS: hamstrings, †: significant group main effect in two-way ANOVA)..... 16

Table 2. 3 Mean and standard deviation of force generating capacity. (CAI: chronic ankle instability group, CON: control group, LAND: landing, ANT: anticipated cutting, UNANT: unanticipated cutting, SL: soleus, MG, medial gastrocnemius, LG: lateral gastrocnemius, TA: tibialis anterior, FL: fibularis longus, VAS: vastus muscles, RF: rectus femoris, GX: gluteus maximus, GM: gluteus medius, HAMS: hamstrings, †: significant group main effect in two-way ANOVA, ‡, §, ¶, #: significant differences in Fisher's LSD post hoc testing)..... 18

CHAPTER 4

Table 4. 1 Principal component (PC) scores (means and standard deviation) for lateral gastrocnemius (LG), medial gastrocnemius (MG), fibularis longus (FL), soleus (SOL), and tibialis anterior (TA) in people with chronic ankle instability (CAI) and for healthy controls (CON) for the landing (Land), anticipated cutting (Ant), and unanticipated cutting (Unant) tasks. 50

CHAPTER 5

Table 5. 1 Cosine-similarity coefficients for each synergy vector comparison (CAI: chronic ankle instability group, CON: healthy control, Ant: anticipated landing-cutting, Unant: unanticipated landing-cutting). 65

Table 5. 2 Zero lag cross-correlation coefficients for each activation coefficient comparison (CAI: chronic ankle instability group, CON: healthy control, Ant: anticipated landing-cutting, Unant: unanticipated landing-cutting)..... 66

LIST OF FIGURES

CHAPTER 2

- Figure 2. 1 Workflow. (IK: inverse kinematics, ***F_{peak}***: peak muscle force, ***F_{iso}***: maximum isometric force, ***a***: activation, ***f_L***: effect of muscle length, ***f_v***: effect of muscle velocity) 13
- Figure 2. 2 Mean and standard deviation of the simulated muscle activations from static optimization and experimental EMG (blue line and shaded area: chronic ankle instability group, red line, and shaded area: control group, green shaded area: measured EMG) 15
- Figure 2. 3 Task-averaged gluteus maximus muscle forces (x body weight) for people with (CAI) and without (CON) chronic ankle instability 17
- Figure 2. 4 Task-averaged gluteus maximus force generating capacity muscle forces for people with (CAI) and without (CON) chronic ankle instability. 19
- Figure 2. 5 Vastii muscle group force generating capacity for people with group (CAI) and without (CON) chronic ankle instability during the landing (LAND), anticipated cutting (ANT), and unanticipated cutting (UNANT) tasks 20

CHAPTER 3

- Figure 3. 1 Workflow. A: scaling of model. B: inverse kinematics (IK). C: static optimization (SO). D: validation by comparing pattern of measured muscle activation and simulated activation. E: joint reaction analysis with all forces (e.g., ground reaction force (GRF) and individual muscle). F: separate joint reaction analysis for each force (e.g., GRF or individual muscle)..... 30
- Figure 3. 2 Mean±SD normalized muscle activations from EMG and simulation in people with chronic ankle instability (CAI) and healthy controls (CON) during unanticipated cutting. SL: soleus, MG: medial gastrocnemius, LG: lateral gastrocnemius, TA: tibialis anterior, FL: fibularis longus. 31
- Figure 3. 3 Mean±SD normalized time-series ankle joint compression force (top) and anteroposterior shear force (bottom) in people with chronic ankle instability (CAI) and healthy controls (CON) during unanticipated cutting..... 33
- Figure 3. 4 Averaged and normalized ankle joint compression (top row) and anteroposterior (bottom row) forces and contributions from ground reaction forces and individual muscles in people with chronic ankle instability (CAI) and healthy controls (CON) during anticipated cutting. JCF: joint contact force, GRF: ground reaction force, SL: soleus, MG: medial gastrocnemius, LG: lateral gastrocnemius, TP: tibialis posterior, TA: tibialis anterior, FB: fibularis brevis, FL: fibularis longus 34

Figure 3. 5 Mean \pm SD normalized contribution of ground reaction force and individual muscles at time of peak ankle joint compression force in people with chronic ankle instability (CAI) and healthy controls (CON) during unanticipated cutting. JCF: joint contact force, GRF: ground reaction force, SL: soleus, MG: medial gastrocnemius, LG: lateral gastrocnemius, TP: tibialis posterior, TA: tibialis anterior, FB: fibularis brevis, FL: fibularis longus..... 35

Figure 3. 6 Mean \pm SD normalized contribution of ground reaction force and individual muscles at time of first anterior, posterior, and second anterior peaks of ankle joint anteroposterior (AP) shear force in people with chronic ankle instability (CAI) and healthy controls (CON) during unanticipated cutting. JCF: joint contact force, GRF: ground reaction force, SL: soleus, MG: medial gastrocnemius, LG: lateral gastrocnemius, TP: tibialis posterior, TA: tibialis anterior, FB: fibularis brevis, FL: fibularis longus, *: significant difference with $p < 0.05$ 36

CHAPTER 4

Figure 4. 1 Time-frequency heatmaps for mean wavelet intensities of the lateral gastrocnemius (first row), medial gastrocnemius (second row), fibularis longus (third row), soleus (fourth row), and tibialis anterior (fifth row) during 200 ms of the landing task (left two columns) and during the stance phases of the anticipated cutting task (middle two columns) and unanticipated cutting task (right two columns)..... 48

Figure 4. 2 Variation in wavelet intensity captured by the two principal components (PC). The effects of positive and negative PC scores on wavelet intensities are illustrated by simulating a one standard deviation (1SD) change in the PC on the mean intensity of the EMG data and can be visualized by the dashed lines and the + and – symbols, respectively. The effects. VAF – variance accounted for by the given PC. 49

Figure 4. 3 Muscle- and task-averaged PC1 scores (i.e., magnitude of the wavelet intensities) for people with chronic ankle instability (CAI) and for people in the control group (CON) 51

Figure 4. 4 Muscle-averaged PC2 scores (i.e., shift in center frequencies of wavelet intensities) for people with chronic ankle instability (CAI) and for people in the control group (CON) during the landing, anticipated cutting, and unanticipated cutting task. 52

CHAPTER 5

Figure 5. 1 Mean \pm SD normalized muscle activity in people with chronic ankle instability (CAI) and healthy controls (CON) during anticipated (Ant) and unant (Unant) cutting. SL: soleus, MG: medial gastrocnemius, LG: lateral gastrocnemius, TA: tibialis anterior, FL: fibularis longus..... 63

Figure 5. 2 Variance accounted for the synergies for each group during each task (CAI: chronic ankle instability group, CON: healthy control, Ant: anticipated landing-cutting, Unant: unanticipated landing-cutting). 65

Figure 5. 3 Muscle synergy vectors (and muscle-specific weightings) and activation coefficients extracted from each group during each task (CAI: chronic ankle instability group, CON: healthy control, Ant: anticipated landing-cutting, Unant: unanticipated landing-cutting, SL: soleus, MG: medial gastrocnemius, LG: lateral gastrocnemius, TA: tibialis anterior, FL: fibularis longus, G: main effect for group, T: main effect for task). 67

CHAPTER 1: INTRODUCTION

About two million people suffer from CAI in the United States each year (Waterman, Owens, Davey, Zacchilli, & Belmont, 2010). In particular, 23.4% of athletes have CAI and therefore display higher risk of recurring lateral ankle sprains (Tanen, Docherty, Van Der Pol, Simon, & Schrader, 2014). Three billion health care dollars are spent annually to treat CAI in the US alone (Radwan et al., 2016). Although a variety of studies have investigated underlying mechanisms associated with CAI, the research on rehabilitation interventions shows that the current intervention protocols are not always successful (O'Driscoll & Delahunt, 2011; Song, Rhodes, & Wikstrom, 2018; Tsikopoulos et al., 2019; Vallandingham, Gaven, & Powden, 2019), and the prevalence of CAI remains high (e.g., 61% of soccer players with CAI) (Attenborough et al., 2014). The lack of success of CAI rehabilitation protocols is important because people with CAI have a higher risk of additional and more serious clinical sequelae, such as ankle osteoarthritis (OA) (Carbone & Rodeo, 2017; Wikstrom, Hubbard-Turner, & McKeon, 2013).

Dynamic movements during sports activities are thought to present primary contributors to the progression of ankle OA (Hunter & Eckstein, 2009) because joint contact forces are greater during dynamic movements than daily life activities, such as walking (Cleather, Goodwin, & Bull, 2013). Recent research reviewed the kinematic characteristics of people with CAI during landing tasks (J. D. Simpson, Stewart, Macias, Chander, & Knight, 2019; Theisen & Day, 2019). Greater dorsiflexion and smaller sagittal plane range of motion in the ankle joint were consistently found during landing tasks (C. Brown, Padua, Marshall, & Guskiewicz, 2008; Caulfield & Garrett, 2002; C. J. Wright, Arnold, & Ross, 2016). Furthermore, less knee flexion was also reported in previous

research (Gribble & Robinson, 2009; Terada, Pietrosimone, & Gribble, 2014; Theisen & Day, 2019). Kinematic differences in people with CAI may also be associated with differences in joint kinetics (J. D. Simpson et al., 2019). For example, less ankle sagittal plane motion during landing may increase the impact force in the knee and hip joints (Doherty et al., 2016; Gribble & Robinson, 2009; Monaghan, Delahunt, & Caulfield, 2006; J. D. Simpson et al., 2019), which suggests that people with CAI also have greater risks of not only sustaining ankle injuries but also knee injuries (Alentorn-Geli et al., 2009). In addition to research on landing motions, cutting motions have also been investigated (Kim, Son, Seeley, & Hopkins, 2019). Kim et al. (2019) reported that patients with CAI had less dorsiflexion, greater knee and hip flexion angles, and greater inversion and hip adduction angles during jump landing-cutting motions (Kim et al., 2019). Overall, these pathologic kinematics in people with CAI during dynamic movements may alter lower extremity kinetics (Monaghan et al., 2006) in a way that increases ankle joint contact forces and precipitates the development of ankle OA. Because pathologic movements originate from abnormal neuromuscular control, it is necessary to investigate neuromuscular deficits in CAI patients in order to help clinicians treat CAI and prevent the progression of ankle OA in this population.

Neuromuscular deficits in people with CAI manifest as differences in muscle function, which have been thoroughly investigated through a variety of experimental designs and technologies such as EMG (Feger, Donovan, Hart, & Hertel, 2015; Flevas et al., 2017; Kwon, Harrison, Kweon, & Blaise Williams, 2019; Son, Kim, Seeley, & Hopkins, 2017), isometric dynamometry (McCann, Terada, Kosik, & Gribble, 2019), or ultrasound (DeJong, Mangum, & Hertel, 2019). Although muscular deficits have been

characterized in people with CAI, the direct role of each muscle in relation to risk factors (e.g., ankle joint contact forces) of ankle OA have not been quantified. A major obstacle is that the contribution of each muscle on ankle joint contact forces cannot be evaluated with traditional experimental studies because of the difficulty of measuring muscle forces directly. This obstacle makes it difficult to identify and target specific muscles during rehabilitation for people with CAI. Computer simulations, however, can provide a tool to estimate both muscle forces and ankle joint contact forces. In addition, these simulations can be used to compute the individual contributions of each muscle to ankle joint contact forces. Therefore, the completion and information gained from Specific Aim 1 and 2 will provide foundational and quantitative guidance about which muscles contribute to known risk factors for ankle OA in people with CAI during dynamic tasks. This may ultimately enhance the efficacy of rehabilitation programs by providing clinicians with detailed knowledge about which muscles should be targeted during rehabilitation. To complete this aim, we will use dynamic neuromusculoskeletal (NMS) simulations, which have not been used in the context of CAI, but provide valuable tools to evaluate patient-specific muscle function by combining experimental data (e.g., motion capture data) with musculoskeletal models.

Electromyography (EMG) has been commonly used to investigate neuromuscular deficits, such as delay (Fleivas et al., 2017), weakness (Son et al., 2017), compensation (Kwon et al., 2019), or longer duration (Feger et al., 2015) of muscle activations in people with CAI. These deficits were found in variables extracted from the time-magnitude domain of traditionally filtered and smoothed EMG data. However, the time-frequency domain of EMG data also contains important information related to motor unit recruitment

strategies of the peripheral nervous system (PNS) (Wakeling, Uehli, & Rozitis, 2006). For example, a previous study revealed the characteristics of multi-muscle activation patterns in the time-frequency domain in people with ankle OA (von Tscharnner & Valderrabano, 2010). Because CAI leads to ankle OA, it is necessary to investigate the muscle activation strategies in the time-frequency domain in people with CAI. Completion of Specific Aim 3 will strengthen the knowledge by revealing different muscle activation strategies in the time-frequency domain in people with CAI.

In addition, CNS control of muscle activation strategies in people with CAI has not been thoroughly investigated. Although some evidence regarding CNS deficits in people with CAI has been reported, this has been primarily in static tasks. For example, Rosen et al. (2019) reported larger variability in cortical activation with the fNIRS in CAI patients compared to healthy controls (A. B. Rosen et al., 2019) and Needle et al. (2013) reported correlations between cortical excitability and ankle laxity with transcranial magnetic stimulation (TMS) (Needle, Palmer, Kesar, Binder-Macleod, & Swanik, 2013). However, the methods used by these authors only allow for the study of CNS deficits during static postures. One way to study CNS control of muscle activation strategies is through the use of muscle synergy analysis. Muscle synergies can be defined as patterns of activation of muscles recruited by a single neural command signal, and have been used to identify CNS deficits of neurologic pathologies such as stroke or cerebral palsy (Allen, Kesar, & Ting, 2019; Shuman, Goudriaan, Desloovere, Schwartz, & Steele, 2019). Non-negative matrix factorization (NMF) is commonly used to estimate muscle synergies (d'Avella, Saltiel, & Bizzi, 2003; D. D. Lee & Seung, 1999). The results from the NMF analysis provides several meaningful insights about CNS control. For example, the number of muscle synergies

provides information about the complexity of an individual's strategies to control movements (Safavynia, Torres-Oviedo, & Ting, 2011), where individuals with less complexity in multi-muscle activations have fewer muscle synergies (Clark, Ting, Zajac, Neptune, & Kautz, 2010). Furthermore, the patterns within each muscle synergy provide information about spatiotemporal characteristics of movement control from the perspective of the CNS (Safavynia et al., 2011). Because CAI is also considered a neurologic pathology (Needle, Lepley, & Grooms, 2017; Needle et al., 2013; A. B. Rosen et al., 2019), it should also be investigated with appropriate methods, such as NMF. Completion of Specific Aim 4 will provide information about CNS control deficits, and about more global aspects of neuromuscular control as opposed to the limited scope of previous investigations of neuromuscular deficits in people with CAI.

Specific aims

Aim 1: Estimate the forces and force generating capacities of individual lower extremity muscles and compare these estimates between people with and without CAI during landing and cutting tasks.

Hypothesis 1: Peak muscle forces and force generating capacities would differ between groups and that these differences would be task-dependent.

Aim 2: Investigate the contributions from muscle forces and ground reaction force to ankle joint compression and anteroposterior shear forces in people with and without CAI during a cutting task.

Hypothesis 2: Ankle joint compression and anteroposterior shear forces would be greater in people with CAI, and that the contribution of specific muscles to these forces would differ.

Aim 3: Identify differences in the time-frequency domain of muscle activation patterns between people with and without CAI during landing, anticipated cutting, and unanticipated cutting.

Hypothesis 3: There would be differences in the frequencies of muscle activation patterns between people with and without CAI and that these differences would be task-dependent.

Aim 4: Investigate and compare CNS-based neuromuscular control strategies in people with CAI and healthy CON during cutting tasks.

Hypothesis 4: People with CAI would use fewer (i.e., less complex) muscle synergies, exhibit different muscle-specific weightings within muscle synergies, and display task-specific these differences in muscle synergies.

CHAPTER 2: PEAK FORCES AND FORCE GENERATING CAPACITIES OF LOWER EXTREMITY MUSCLES DURING DYNAMIC TASKS IN PEOPLE WITH AND WITHOUT CHRONIC ANKLE INSTABILITY

INTRODUCTION

Ankle ligament sprains are common musculoskeletal injuries and occur when the angles of talocrural or subtalar joints are excessively large and the forces within the ligaments increase beyond their maximal capacity. People who sprain their ankle ligaments may develop chronic ankle instability (CAI) (Gribble et al., 2016). People with CAI experience recurrent ankle sprains because of mechanical deficits (e.g., malalignment (Caputo et al., 2009), laxity (Hubbard-Turner, 2012), and restricted dorsiflexion (Tabrizi, McIntyre, Quesnel, & Howard, 2000)) and neuromuscular deficits (e.g., proprioceptive errors (Munn, Sullivan, & Schneiders, 2010), delayed activations (Hoch & McKeon, 2014), and diminished H-reflex (Hopkins, Brown, Christensen, & Palmieri-Smith, 2009)) in the ankle joint. Furthermore, recent studies reported people with CAI have a substantially higher risk of developing ankle osteoarthritis because the aforementioned deficits can damage the articular surfaces in the talocrural joint (Valderrabano, Hintermann, Horisberger, & Fung, 2006; Valderrabano, Horisberger, Russell, Dougall, & Hintermann, 2009). Although researchers and clinicians have developed rehabilitation protocols to combat the negative effects of CAI, rehabilitation outcomes are not always successful (O'Driscoll & Delahunt, 2011; Song et al., 2018; Tsikopoulos et al., 2019; Vallandingham et al., 2019), which suggests that the mechanisms and deficits in neuromuscular function are not fully understood or that they are not being adequately targeted within rehabilitation programs.

Previous studies have investigated neuromuscular characteristics in people with CAI with a variety of experimental research methods (Feger et al., 2015; Kim et al., 2019; Jeffrey D Simpson et al., 2020; Suttmiller & McCann, 2020; Willems, Witvrouw, Verstuyft, Vaes, & De Clercq, 2002; Wisthoff et al., 2019). For example, electromyography (EMG) has been used to record and compare muscle activation between people with CAI and matched controls (Feger et al., 2015; Kim et al., 2019; Jeffrey D Simpson et al., 2020; Suttmiller & McCann, 2020). Results from these studies suggest that people with CAI exhibited greater muscle activation of tibialis anterior during a side-cutting task (Jeffrey D Simpson et al., 2020) and greater muscle activation of medial gastrocnemius during jump landing-cutting motions (Kim et al., 2019). Furthermore, EMG recordings of electrically evoked potentials revealed that people with CAI exhibit a greater decrease in spinal reflex excitability (i.e., Hoffmann reflex) of the soleus when transitioning from bipedal to unipedal stance (Suttmiller & McCann, 2020). In addition, investigations of muscle activation timing relative to initial contact during walking revealed that people with CAI exhibited earlier activations in anterior tibialis, peroneus longus, lateral gastrocnemius, rectus femoris, biceps femoris, and gluteus medius muscles than people without CAI (Feger et al., 2015). Moreover, dynamometry has been used to investigate strength of ankle muscles in people with CAI (Willems et al., 2002; Wisthoff et al., 2019). For example, people with CAI exhibited lower concentric strength of plantar flexor (Wisthoff et al., 2019) and lower muscle strength of evtor during isokinetic contraction test (Willems et al., 2002). Although neuromuscular differences between people with CAI and healthy controls are well characterized, less is known about forces and activations of deeper muscles or about the function of individual

muscles as people with CAI perform dynamic tasks because of limitations associated with measurements of superficial muscles (e.g., soleus) from surface EMG.

Although studies have investigated muscle activation and function via EMG in people with CAI, no previous studies have investigated the force-length-velocity behavior of individual muscles during functional dynamic tasks, such as jumping or cutting, in this population. A major obstacle for experimental studies that use EMG is that they do not provide information about the forces and length changes of multiple muscles during dynamic tasks. Computer simulations and musculoskeletal modeling, however, provide tools to estimate the kinematics and kinetics of individual muscles. These tools allow for the dynamic estimation of a muscle's peak force, and even its force-length (f_L) and force-velocity (f_v) behavior during any given task as long as the instantaneous joint kinematics (e.g., joint angle and angular velocity) are also known (Arnold, Hamner, Seth, Millard, & Delp, 2013). Further, this information can also be used to estimate a muscle's instantaneous force generating capacity, which allows us to better understand the "relative" ability or capacity of a muscle to produce force and thus complements the analysis of "absolute" peak muscle forces, which is more traditional.

Therefore, the purpose of this study was to estimate the forces and force generating capacity of individual lower extremity muscles and to compare these estimates between people with and without CAI during landing and cutting tasks. We hypothesized that the peak muscle forces and force generating capacity would differ between groups and that these differences would be task dependent.

METHODS

Participants

Twenty-two subjects (11 healthy people and 11 CAI) participated in this study (Table 2. 1). A questionnaire was used for inclusion into the CAI group by quantifying history of ankle sprains and symptoms of the ankle joint (Kipp & Palmieri-Smith, 2013; McVey, Palmieri, Docherty, Zinder, & Ingersoll, 2005). In addition, the Foot & Ankle Disability Index (FADI) (Intraclass correlation coefficients (ICC) = 0.93) and FADI – Sports (ICC = 0.92) questionnaire were used to quantify general and sports-related functional deficits, respectively (Hale & Hertel, 2005). People in the control group (CON) were matched by sex, age, height, weight, and physical activity level, which was quantified via Tegner scores (ICC = 0.8) (Briggs et al., 2009).

Table 2. 1 Demographic information. (CAI: chronic ankle instability group, CON: control group, FADI: Foot & Ankle Disability Index, FADIS: Foot & Ankle Disability Index in Sports, Tegner: Tegner’s score)

Group	Year	Height (m)	Weight (kg)	FADI (%)	FADIS (%)	Tegner
CAI	22.1 ± 3.2	1.68 ± 0.11	69.0 ± 19.1	90.3 ± 9.4	88.6 ± 9.1	5.3 ± 1.2
CON	22.6 ± 4.2	1.74 ± 0.11	66.8 ± 15.5	100 ± 0.0	100 ± 0.0	5.3 ± 1.0

Data collection

The subjects performed three tasks (landing, anticipated cutting, unanticipated cutting) with reflective markers attached to the skin over bony landmarks on the pelvis, femur, tibia, and foot segments (T. N. Brown, Palmieri-Smith, & McLean, 2009; Kipp & Palmieri-Smith, 2012) and 5 EMG electrodes attached over the soleus, fibularis longus, tibialis anterior, medial gastrocnemius, and lateral gastrocnemius muscles. For the

landing task (LAND), subjects were asked to perform a forward-jump over a 15 cm box and land on a force plate on a single leg. The forward-jump distance was set to the subject's leg length. For the anticipated and unanticipated cutting tasks, subjects performed the same forward jump, but subsequently also performed a 90° cut immediately after landing on the force plate. The cutting direction was indicated with a light stimulus, which was turned on 5 sec before jumping during the anticipated condition (ANT). For unanticipated cutting (UNANT) the light stimulus came on when subjects passed through a light beam that was set halfway between the starting position and the force plate. Three-dimensional position of markers, muscle activations, and ground reaction forces (GRF) were collected with motion capture cameras (ViconMx, CA, USA), an EMG system (Bagnoli, Delsys, MA, USA), and a force platform (Advanced Medical Technologies Inc., MA, USA). Sampling frequencies were set to 240 Hz for the cameras and to 1200 Hz for the EMG system and force platform of which data was amplified).

Data processing

Three-dimensional marker positions and GRFs were filtered with lowpass Butterworth filters at cutoff frequencies of 12 Hz. The EMG data were bandpass-filtered with Butterworth filters at cutoff frequencies of 20 and 450 Hz. The filtered EMG data was rectified and smoothed with a lowpass Butterworth filter at cutoff frequency of 10 Hz to obtain an EMG envelope. Then, each EMG signal envelope was normalized by the maximum value of the signal (Lai, Schache, Brown, & Pandy, 2016). All data were time-normalized to 0-100 % of task duration (i.e., 200 ms for the landing task and stance phase for cutting tasks).

A musculoskeletal model with 23 degree-of-freedom and 92 muscle actuators was scaled to data from a static trial for each subject (Delp et al., 1990). Scaling created a subject-specific model and considered each subject's individual geometry (e.g., segment size, segment mass, or muscle lengths) (Figure 2. 1.A). Since the dynamic muscle forces of the generic model were too low to perform the dynamic tasks in the current study, the maximum isometric muscle forces of each subject were scaled by a generic ($\times 3$) and a subject-specific constant that was based on estimates of lower extremity muscle volume (Handsfield, Meyer, Hart, Abel, & Blemker, 2014). Lower extremity muscle volumes were estimated based on regression model (Equation 1) (Handsfield et al., 2014).

$$\text{Volume of lower extremity muscles} = (47 \times \text{Body mass} \times \text{Height}) + 1285$$

(Equation 1)

The inverse kinematics (IK) tool was used to calculate joint angles by minimizing differences between virtual model markers and experimental subject markers (Figure 2. 1.B). Static optimization (SO) was used to estimate muscle forces and activations from GRF and joint angle data. SO estimates the activation for each muscle by finding the combination of activations that minimizes the sum of squared activations of all muscles to match the sum of muscle moments to inverse dynamic based net joint moments. Then, SO estimates force for each muscle by multiplying maximal isometric muscle force, estimated activation, multipliers from force-length-velocity relationship. (Figure 2. 1.C). All analyses with a musculoskeletal model were performed with OpenSim (Delp et al., 2007).

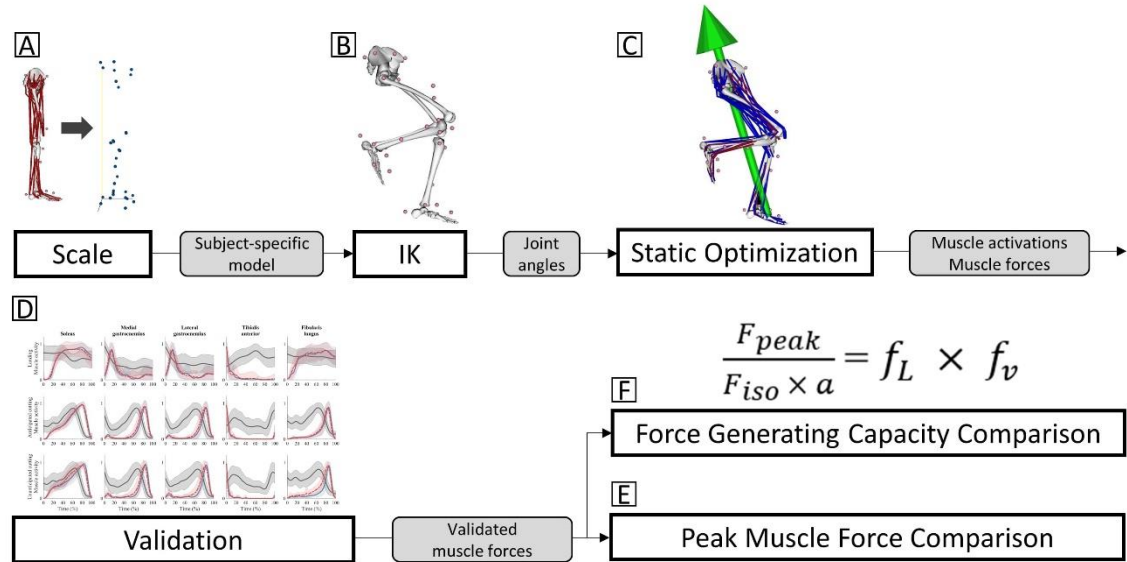


Figure 2. 1 Workflow. (IK: inverse kinematics, F_{peak} : peak muscle force, F_{iso} : maximum isometric force, a : activation, f_L : effect of muscle length, f_v : effect of muscle velocity)

Muscle forces from the soleus, medial gastrocnemius, lateral gastrocnemius, tibialis posterior, tibialis anterior, fibularis longus, fibularis brevis, vastus lateralis / medialis / intermedius (grouped together), rectus femoris, superior / middle / inferior fibers of gluteus maximus (grouped together), anterior / middle / posterior fibers of gluteus medius (grouped together), biceps femoris long and short heads / semimembranosus / semitendinosus (grouped together) were calculated and used for statistical analyses. Peak muscle forces from each trial were extracted and normalized by each subject's body weight (BW) (Figure 2. 1.E). In addition, the force generating capacity of each muscle group was calculated by dividing peak muscle force (F_{peak}) by the maximum isometric force (F_{iso}) and concurrent activation (a) (Figure 2. 1.F), which also accounts for the effects of muscle length (f_L) and velocity (f_v) (Equation 2) (Arnold et al., 2013). A greater force generating capacity indicates that a muscle requires less activation to produce the same amount of muscle force.

$$\text{Force generation capacity} = \frac{F_{peak}}{F_{iso} \times a} = f_L \times f_v \quad (\text{Equation 2})$$

EMG data were used to validate the simulated muscle activity from static optimization (Hicks, Uchida, Seth, Rajagopal, & Delp, 2015). Given the absence of maximum voluntary isometric contractions for all muscles, the experimental and simulated EMG data were normalized to the peak value during the dynamic trials and visually compared based on the temporal pattern of muscle activity (Figure 2. 1.D) (Hamner & Delp, 2013; Hamner, Seth, & Delp, 2010).

Statistical analysis

Separate two-way analyses of variance (ANOVA) were used to compare peak muscle forces and force generating capacity of each muscle and muscle group. The independent variables were group (CAI and CON) and task (LAND, ANT, and UNANT). Significant interaction or main effects were followed by Fisher's least significant difference (LSD) procedure to examine pair-wise differences during post-hoc testing. The alpha level for each ANOVA was set to 0.05. Omega-Squared (ω^2) effect-sizes were also calculated (Equation 3).

$$\omega^2 = \frac{SS_{factor} - df_{factor} \cdot MS_{error}}{SS_{total} + MS_{error}} \quad (\text{Equation 3})$$

The ω^2 was considered as very small if between 0-0.01, small if between 0.01-0.06, medium if between 0.06-0.14, and large if greater than 0.14 (Field, 2013). All statistical analyses were performed in MATLAB (MathWorks, MA, USA).

RESULTS

Considering electromechanical delay (Corcos, Gottlieb, Latash, Almeida, & Agarwal, 1992), the simulated EMG data exhibited similar patterns as the experimental EMG data during all tasks and therefore appear to valid for further analysis and processing (Figure 2. 2) (Hicks et al., 2015).

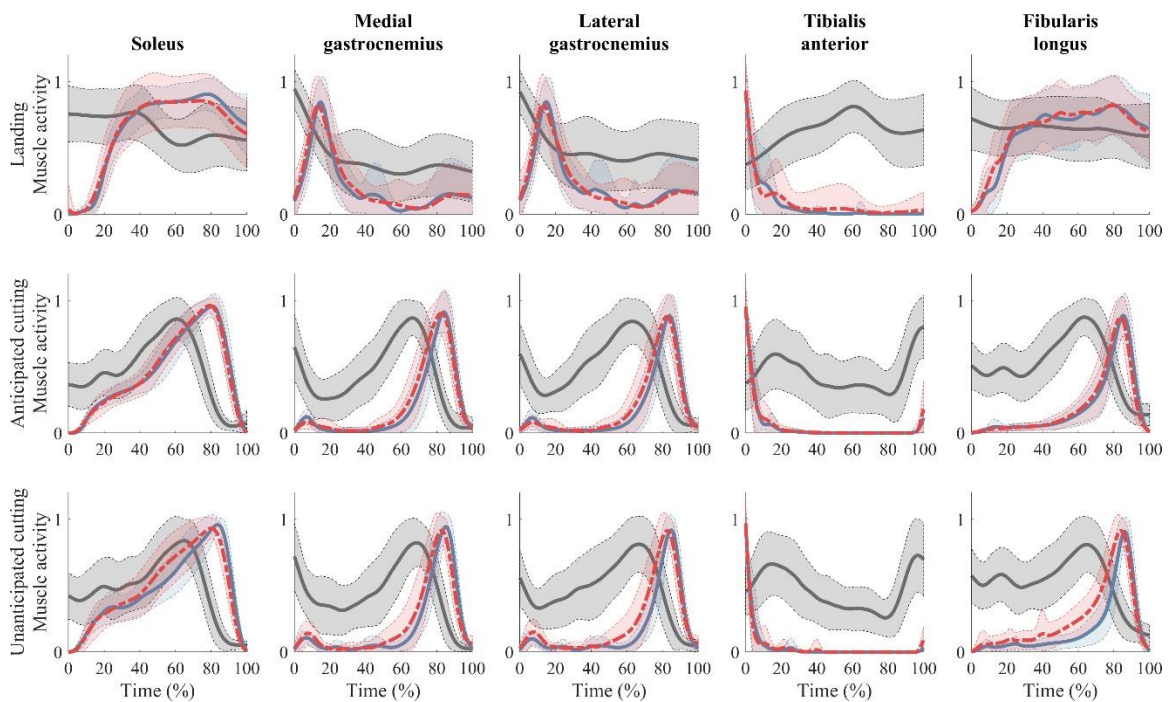


Figure 2. 2 Mean and standard deviation of the simulated muscle activations from static optimization and experimental EMG (blue line and shaded area: chronic ankle instability group, red line, and shaded area: control group, green shaded area: measured EMG)

There were no significant group by task interactions for any peak muscle forces. However, there was a significant group main effect ($p = 0.018$) and medium effect size ($\omega^2 = 0.08$) for peak gluteus maximus force (Table 2. 2 and Figure 2. 3). Specifically, the CAI group generated greater peak gluteus maximus forces during all tasks.

Table 2. 2 Mean and standard deviation of muscle force. (CAI: chronic ankle instability group, CON: control group, LAND: landing, ANT: anticipated cutting, UNANT: unanticipated cutting, SL: soleus, MG, medial gastrocnemius, LG: lateral gastrocnemius, TA: tibialis anterior, FL: fibularis longus, VAS: vastus muscles, RF: rectus femoris, GX: gluteus maximus, GM: gluteus medius, HAMS: hamstrings, †: significant group main effect in two-way ANOVA)

Muscle	Muscle Force (BW)								Two-way ANOVA					
	CAI			CON			Group		Interaction	Group		Task		
	LAND	ANT	UNANT	LAND	ANT	UNANT	CAI	CON		<i>p</i>	ω^2	<i>p</i>	ω^2	<i>p</i>
SL	4.69±0.78	5.50±1.10	6.04±1.20	4.32±1.23	5.79±0.94	5.80±0.87	5.37±1.14	5.30±1.21	0.560	0.01	0.687	0.01	0.001	0.25
MG	1.20±0.34	1.55±0.29	1.78±0.53	1.05±0.37	1.59±0.38	1.45±0.28	1.49±0.45	1.37±0.41	0.297	0.01	0.133	0.02	0.001	0.25
LG	0.29±0.09	0.37±0.11	0.47±0.21	0.26±0.10	0.39±0.15	0.37±0.13	0.37±0.15	0.34±0.14	0.353	0.00	0.308	0.00	0.003	0.16
TA	0.20±0.10	0.18±0.07	0.24±0.11	0.28±0.19	0.14±0.06	0.26±0.13	0.20±0.10	0.23±0.15	0.335	0.00	0.464	0.01	0.025	0.09
FL	0.14±0.18	0.76±0.33	0.95±0.49	0.10±0.07	0.85±0.52	0.60±0.27	0.59±0.48	0.52±0.46	0.136	0.02	0.268	0.00	0.001	0.44
VAS	6.98±0.88	7.49±0.76	8.13±1.43	6.66±1.41	8.20±1.82	8.42±2.11	7.49±1.10	7.76±1.91	0.522	0.01	0.543	0.01	0.008	0.13
RF	1.35±0.41	1.11±0.53	1.87±0.97	1.70±0.64	1.28±0.24	1.58±0.44	1.42±0.70	1.52±0.49	0.201	0.02	0.605	0.01	0.016	0.10
GX	1.77±0.64	1.70±0.61	1.92±0.73	1.33±0.38	1.46±0.49	1.54±0.52	1.79±0.64 [†]	1.44±0.46 [†]	0.843	0.03	0.018	0.08	0.579	0.01
GM	3.31±0.53	2.48±0.69	3.09±1.04	3.19±0.51	2.39±0.60	2.90±0.87	2.95±0.82	2.83±0.73	0.976	0.03	0.479	0.01	0.002	0.17
HAMS	1.24±0.39	1.68±0.30	1.99±0.69	1.16±0.27	1.53±0.54	1.91±0.54	1.61±0.55	1.53±0.55	0.963	0.02	0.394	0.00	0.001	0.29

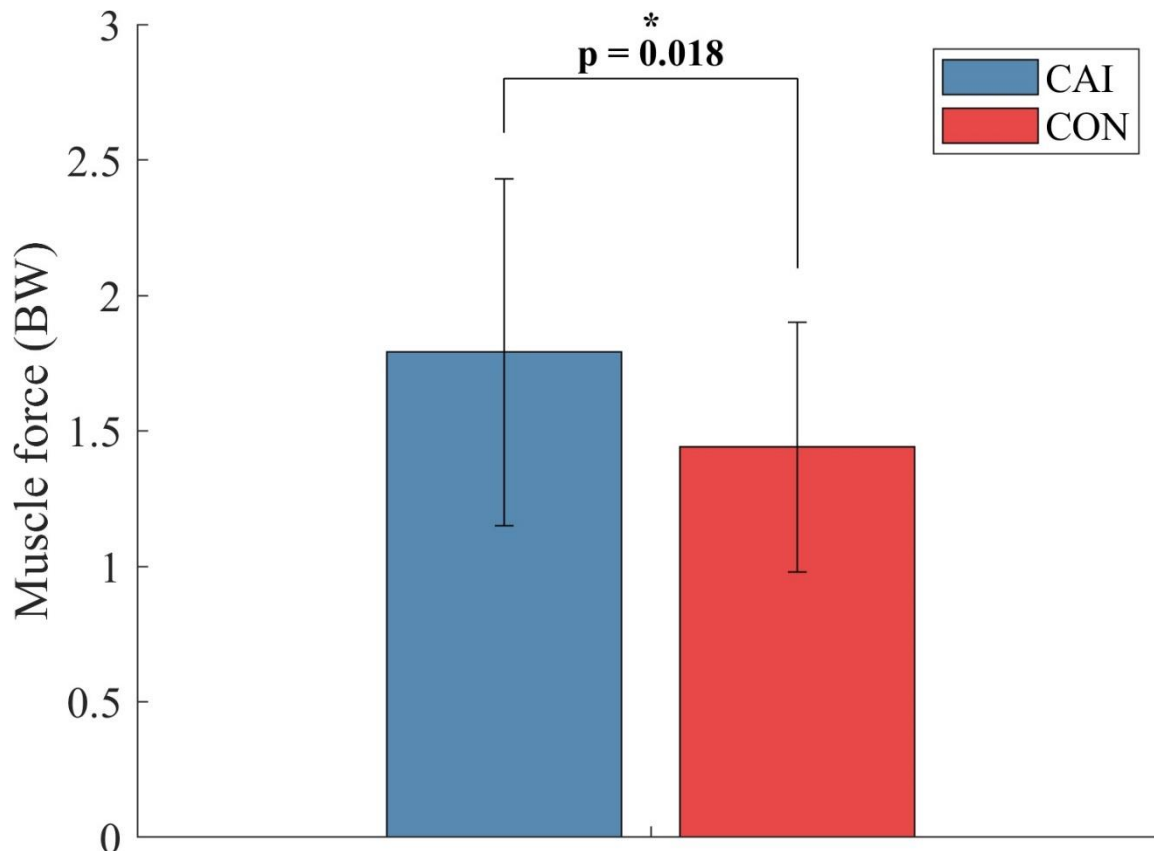


Figure 2. 3 Task-averaged gluteus maximus muscle forces (x body weight) for people with (CAI) and without (CON) chronic ankle instability

There was a significant group by task interaction ($p = 0.009$) with medium effect size ($\omega^2 = 0.11$) for force generating capacity of vastii (Table 2. 3). Fisher's post hoc test revealed that force generating capacity of vastii was significantly greater in CAI group compared to the CON group during UNANT ($p = 0.001$) (Table 2. 3 and Figure 2. 5). Furthermore, there was a significant group main effect ($p = 0.021$) with medium effect size ($\omega^2 = 0.06$) for force generating capacity of gluteus maximus (Table 2. 3 and Figure 2. 4). Specifically, force generating capacity of gluteus maximus was significantly greater in CAI group compared to the CON group regardless of task.

Table 2. 3 Mean and standard deviation of force generating capacity. (CAI: chronic ankle instability group, CON: control group, LAND: landing, ANT: anticipated cutting, UNANT: unanticipated cutting, SL: soleus, MG, medial gastrocnemius, LG: lateral gastrocnemius, TA: tibialis anterior, FL: fibularis longus, VAS: vastus muscles, RF: rectus femoris, GX: gluteus maximus, GM: gluteus medius, HAMS: hamstrings, †: significant group main effect in two-way ANOVA, ‡, §, ¶, #: significant differences in Fisher's LSD post hoc testing)

Muscle	Force generating capacity									Two-way ANOVA						
	CAI			CON			Group			Interaction		Group		Task		
	LAND	ANT	UNANT	LAND	ANT	UNANT	CAI	CON		<i>p</i>	ω^2	<i>p</i>	ω^2	<i>p</i>	ω^2	
SL	1.34±0.08	0.95±0.25	1.08±0.15	1.36±0.12	0.92±0.14	0.98±0.16	1.13±0.24	1.08±0.24		0.506	0.01	0.34	0.10	0.010	0.0010	0.55
MG	1.29±0.11	0.52±0.28	0.77±0.40	1.20±0.14	0.49±0.28	0.85±0.38	0.86±0.43	0.85±0.40		0.668	0.01	0.87	0.10	0.010	0.0010	0.54
LG	1.38±0.11	0.54±0.33	0.80±0.47	1.29±0.15	0.48±0.32	0.95±0.45	0.91±0.48	0.91±0.46		0.492	0.01	0.99	0.10	0.010	0.0010	0.52
TA	0.55±0.07	0.66±0.18	0.53±0.07	0.62±0.12	0.68±0.17	0.55±0.12	0.59±0.13	0.62±0.14		0.765	0.02	0.26	0.10	0.008	0.010	0.13
FL	1.26±0.17	0.61±0.25	0.62±0.18	1.34±0.18	0.54±0.05	0.69±0.17	0.84±0.37	0.86±0.38		0.348	0.01	0.53	0.10	0.010	0.0010	0.78
VAS	1.45±0.07 [‡]	1.37±0.15 [¶]	1.48±0.09 ^{¶#}	1.46±0.08 [§]	1.38±0.12	1.29±0.16 ^{‡§#}	1.43±0.12	1.38±0.14		0.009	0.11	0.06	0.10	0.040	0.080	0.04
RF	1.46±0.18	1.25±0.34	1.50±0.16	1.34±0.19	1.30±0.27	1.49±0.13	1.40±0.26	1.38±0.21		0.504	0.01	0.67	0.10	0.012	0.010	0.11
GX	1.08±0.18	0.91±0.07	0.97±0.14	0.95±0.16	0.84±0.15	0.90±0.14	0.99±0.15 [†]	0.90±0.15 [†]		0.768	0.02	0.02	0.10	0.060	0.011	0.11
GM	1.28±0.12	1.08±0.17	1.11±0.18	1.25±0.07	1.01±0.10	1.06±0.12	1.16±0.17	1.11±0.14		0.846	0.02	0.16	0.10	0.010	0.010	0.34
HAMS	0.72±0.09	0.88±0.10	0.81±0.12	0.69±0.06	0.82±0.15	0.78±0.07	0.80±0.12	0.76±0.11		0.859	0.02	0.11	0.10	0.020	0.0010	0.23

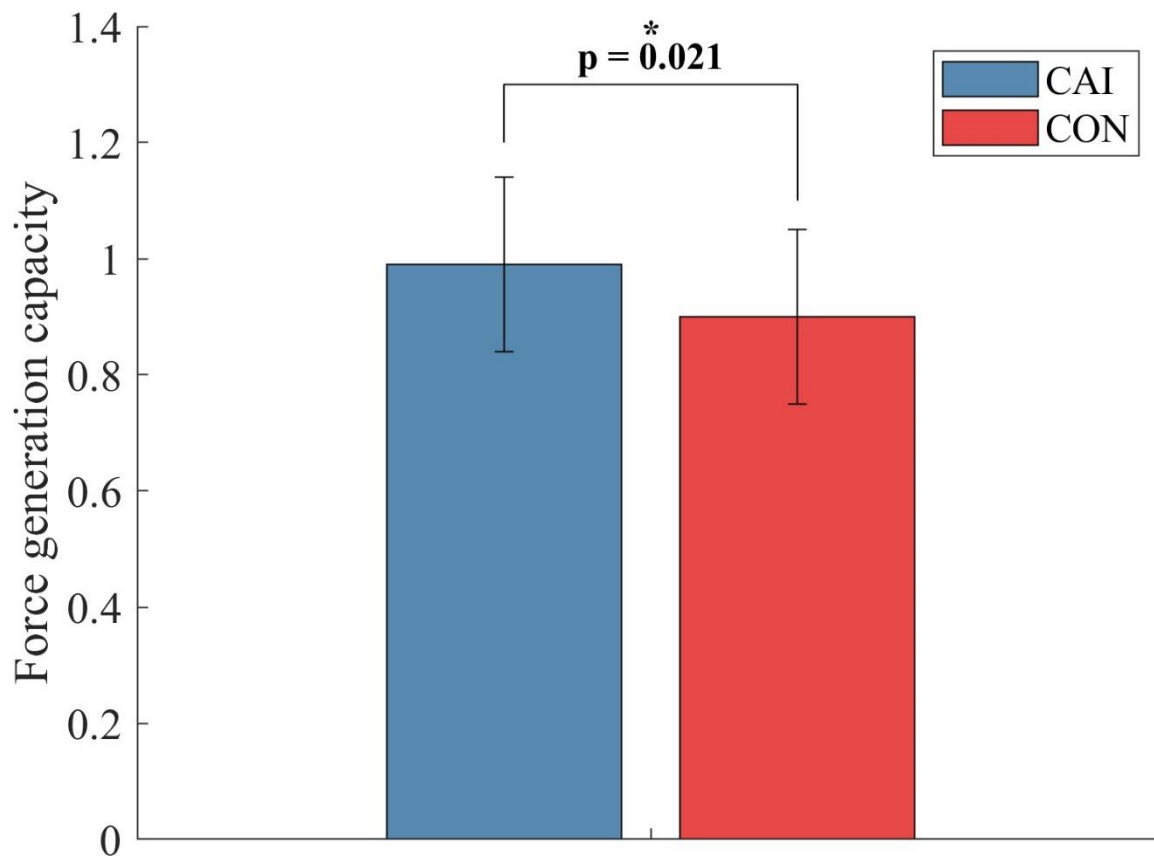


Figure 2. 4 Task-averaged gluteus maximus force generating capacity muscle forces for people with (CAI) and without (CON) chronic ankle instability.

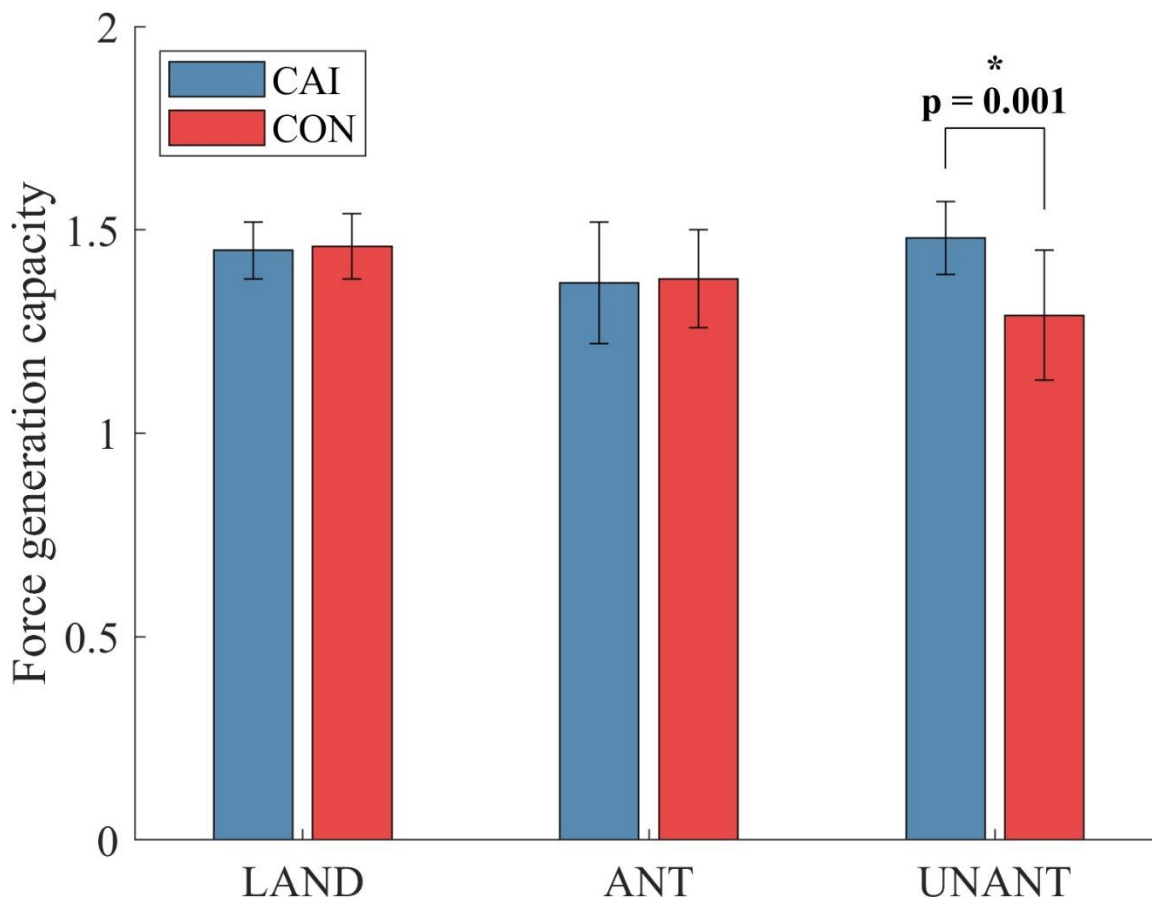


Figure 2. 5 Vastii muscle group force generating capacity for people with group (CAI) and without (CON) chronic ankle instability during the landing (LAND), anticipated cutting (ANT), and unanticipated cutting (UNANT) tasks

DISCUSSION

The purpose of the current study was to estimate peak forces and force generating capacity of lower extremity muscles and to compare these estimates between a group of people with CAI and a healthy control group as they both performed landing and cutting tasks. The results showed that people with CAI exhibited greater peak gluteus maximus muscle forces and a greater capacity to generate gluteus maximus force than people in the CON group across all tasks. In addition, the CAI group also exhibited greater vastii force generating capacity than the CON group during the unanticipated cutting task. Together,

these results partially supported our hypotheses that people with CAI would exhibit different peak muscle forces and force generating capacity, and that these differences would depend on the respective task.

A primary finding of the current study was that people with CAI generated greater peak gluteus maximus forces than people in the CON group across all tasks. More specifically, people with CAI generated on average approximately 24% greater peak gluteus maximus forces during all landing and cutting tasks. This finding agrees with previous studies, which reported that people with CAI exhibit compensatory muscle activations at proximal joints (DeJong, Mangum, & Hertel, 2020; Kim et al., 2019; Rios, Gorges, & dos Santos, 2015). For example, Kim et al. (2019) observed greater activations of knee and hip joint muscles (e.g., vastus lateralis, adductor longus, gluteus maximus, and gluteus medius) in CAI patients during the transition phase (i.e., after landing and before takeoff) of landing/cutting tasks (Kim et al., 2019). Similarly, Rios et al. (2015) reported that people with CAI activated muscles at proximal joints more during the single-leg stance phase of ball-kicking tasks than a group of healthy controls (Rios et al., 2015). Furthermore, DeJong et al. (2020) observed that the difference in ultrasound-based gluteus maximus muscle thickness, which is a purported surrogate of muscle activation, between resting and exercise conditions during a dynamic balance task were greater in a group of people with CAI than a group of healthy controls (DeJong et al., 2020; Mangum, Henderson, Murray, & Saliba, 2018). The authors of these studies suggested that people with CAI adopt greater activation of proximal muscles as a compensatory postural control strategy to mitigate neuromuscular deficits at the ankle joint (DeJong et al., 2020; Kim et al., 2019; Rios et al., 2015). However, since muscle activation assessed via EMG or

ultrasound only provide indirect, and somewhat tenuous, information about muscle forces the results of the current study provide more direct evidence that compensatory muscle function in people with CAI also extends to the generation of force in proximal muscles. Collectively, these findings therefore suggest that people with CAI exhibit neuromuscular differences in the function of proximal muscles, which may reflect a strategy to compensate for deficits at the ankle joint.

Another finding of the current study was that people with CAI exhibited an approximately 10% greater gluteus maximus force generating capacity during all tasks. Given that a muscle's force generating capacity results from the interaction of the force-length (f_L) and force-velocity (f_v) behavior that it exhibits during dynamic tasks, the above result indicates that people with CAI performed all landing and cutting tasks with the gluteus maximus operating closer to its optimal length and/or with slower shortening velocities than people in the CON group. It is thus likely that people with CAI generated greater gluteus maximus force because their chosen movement strategy allowed them to operate at a greater force generating capacity. It is also interesting to note that people with CAI exhibited an approximately 15% greater force generating capacity of vastii, but only during the UNANT task. In contrast to the results about group differences in the gluteus maximus force generating capacity, the difference in force generating capacity of the vastii muscles between groups therefore appears to be task-dependent. The task-dependent difference in force generating capacity likely indicates that during unanticipated tasks, people with CAI alter their movement strategy to allow them to increase the force generating capacity of the vastii, in addition to that of the gluteus maximus, in order to compensate for the uncertainty that is inherent in this task. Although the difference in vastii

force generating capacity did not lead to changes in peak vastii muscle force, it may still be a part of a compensatory strategy that people with CAI use to mitigate neuromuscular deficits at the ankle joint.

We acknowledge several limitations and provide considerations for future study. First, the markers that were used to define the foot segment in the current study were attached to the outside of the participant's shoes, and it is acknowledged that movement of these markers may not directly represent movement of the foot segment. Second, we assumed that the foot segment is one rigid body in this study. However, single-segment foot models may not adequately represent the exact kinematics of the ankle joint (Kim & Kipp, 2019). The use of multi-segment foot model can be used for better capturing foot and ankle movement for the future study. Third, the validation of simulated muscle activations involved only five ankle muscles and did not include proximal muscles. However, the cost function of the SO algorithm minimizes the sum of squared activations of all muscles (proximal and distal), and all estimates fell within reasonable ranges. Although previous research suggests that results from the SO algorithm provides a better match with experimental data than other algorithms (Karabulut et al., 2019), future studies should consider collecting EMG from other muscles for a more comprehensive validation of simulated results. Fourth, the force generating capacity calculation does not provide the detailed information about which of muscle length or shortening velocity makes group differences because it does not calculate multipliers separately from force-length and force-velocity relationship. This limitation suggests that future study should consider the separate analysis of multipliers from force-length and force-velocity relationship to show the detailed muscle behaviors.

CONCLUSION

The current study bolsters the evidence of neuromuscular deficits and task-specific compensatory movement strategies in CAI patients during dynamic movements. Compensatory movement strategies in the CAI patients, such as a “proximal dominant landing strategy”, have been reported in previous studies based on EMG or joint kinematic/kinetic findings (Kim et al., 2019). The current findings provide additional evidence that previously observed disparities in muscle function also extend to differences in muscle forces and force generation capacities (i.e., force-length-velocity behavior) of proximal muscles, and should thus also be considered part of a compensatory landing strategy, in people with CAI. Because compensatory function of proximal muscles suggested that people with CAI exhibited greater muscles force and larger force generation capacities, future research about CAI rehabilitation interventions that aim to prevent recurrent injuries should consider training proximal movement patterns (e.g., kinematic profile) rather than only strengthening muscles, especially during dynamic tasks that include unanticipated decision making elements.

CHAPTER 3: MUSCLE FORCE CONTRIBUTIONS TO ANKLE JOINT CONTACT FORCES DURING AN UNANTICIPATED CUTTING TASK IN PEOPLE WITH CHRONIC ANKLE INSTABILITY

INTRODUCTION

More than 70% of people who suffer a sprain of the lateral ligaments of the ankle joint develop chronic ankle instability (CAI) (Gribble et al., 2016). Based on the current model of CAI and its causes (Hertel & Corbett, 2019), the deficits associated this pathology can be categorized into three main categories of impairments i.e., pathomechanical (e.g., ankle joint laxity (Hubbard-Turner, 2012), limited dorsiflexion (Yoon, Hwang, An, & Oh, 2014)), sensory-perceptual (e.g., impaired proprioception (Willems et al., 2002)), and motor-behavioral (e.g., delayed muscle activation (Fleivas et al., 2017), diminished H-reflex (K.-M. Kim, Ingersoll, & Hertel, 2012)). In combination, these impairments manifest as recurrent ankle sprains, feelings of ‘giving way’ or instability, pain, and swelling all of which decreases the levels of physical activity and quality of life in people with CAI (Houston, Van Lunen, & Hoch, 2014).

The functional impairments that characterize CAI appear to be associated with damage of the articular surface of the talocrural joint at the distal end of the tibia, which is more commonly damaged than the articular surfaces between the talus and the medial and lateral malleoli, and may be the reason that people with CAI have a significantly higher risk of developing ankle osteoarthritis (Carbone & Rodeo, 2017). The occurrence of ankle osteoarthritis in people with CAI is approximately 70% (Hintermann, Boss, & Schafer, 2002). One of the purported risk factors for the development and progression of osteoarthritis is the magnitude of the joint contact force. With respect to the ankle joint,

simulation studies show that joint contact forces and stress increased in the presence of ankle ligament rupture or ankle joint malalignment (Bae, Park, Seon, & Jeon, 2015; Kim & Kipp, 2020). Although the results of these studies have clinical implications about the influence of ankle joint integrity on joint loading, the results were based on simulations and data collected from healthy participants, and not from people with CAI. Only one recent study investigated joint loads in people with CAI (Li, Wang, & Simpson, 2019). That study, however, investigated differences in knee joint contact forces between people with and without CAI and found that both groups exhibited comparable tibiofemoral contact forces during a drop landing on a tilted surface. Although this study provides evidence that CAI does not affect contact forces at proximal joints (Li et al., 2019), which is clinically relevant for musculoskeletal injuries secondary to CAI (e.g., ACL injury), the effects of CAI on contact forces in the ankle joint are still not known. Furthermore, given that joint contact forces are the result of ground reaction forces (GRF) (Wang, Ma, Hou, & Lam, 2017) and muscle forces (W. Herzog, Longino, & Clark, 2003; Sasaki & Neptune, 2010), investigating their respective contributions to the joint contact forces in people with CAI may identify specific muscles that could be targeted during CAI rehabilitation to restore normal loading environment and possibly prevent the onset and progression of ankle osteoarthritis. Investigating the individual contributions from specific muscles and the GRF to the joint contact forces would therefore fill a clinically important research gap.

Therefore, the purpose of this study was to investigate the contributions from muscle forces and GRF to ankle joint compression and anteroposterior shear forces in people with and without CAI during a cutting task. We hypothesized that the ankle joint

compression and anteroposterior shear forces would be greater in people with CAI, and that the contribution of specific muscles to these forces would differ.

METHODS

Participants

Twenty-two participants (11 people with CAI group: 22.1 ± 3.2 years old, 1.68 ± 0.11 m, 69.0 ± 19.1 kg, 11 healthy controls (CON): 22.6 years old, 1.74 ± 0.11 m, 66.8 ± 15.5 kg) participated in this study. Inclusion criteria for the CAI group were based on a modified ankle instability instrument (Hale & Hertel, 2005; Kipp & Palmieri-Smith, 2013; McVey et al., 2005). A group of healthy controls were matched to the CAI group by sex, age, height, weight, and physical activity level, which was based on Tegner scores. The Foot & Ankle Disability Index (FADI) (CAI: 90.3 ± 9.4 ; CON: 100 ± 0.0) and Foot & Ankle Disability Index in Sports (FADIS) (CAI: 88.6 ± 9.1 ; CON: 100 ± 0.0) were used to assess functional ability.

Data collection and experimental protocol

All participants were outfitted with 32 reflective skin markers attached to their pelvis (anterior superior iliac spine, posterior superior iliac spine, iliac crest), femur (greater trochanter, medial and lateral epicondyle, anterior thigh), tibia (fibular head, lateral shank, medial and lateral malleoli), and foot (calcaneal tuberosity, 1st metatarsal base and head, 5th metatarsal head) (T. N. Brown et al., 2009; Kipp & Palmieri-Smith, 2012) and 5 EMG electrodes attached over the muscle bellies of the soleus, medial gastrocnemius, lateral gastrocnemius, tibialis anterior, and fibularis longus muscles.

Each participant was asked to perform three to five successful trials of unanticipated cutting. For this task, participants stood one leg length away from a landing area. Each participant performed a forward jump over a 15 cm box, landed on a single leg, and immediately executed a 90° cut away from the landing leg. The landing leg and cutting direction were indicated by a visual stimulus that was displayed on a computer screen that was set at waist level just behind the force plate. The stimulus was triggered by the breaking of a light beam, which was positioned at the mid-point between the takeoff and position and the landing area (Kim, Palmieri-Smith, & Kipp, 2020). Three-dimensional positions of the reflective markers were collected with motion capture cameras (ViconMx, CA, USA) at a sampling frequency of 240 Hz. Muscle activations were recorded with a Bagnoli electromyography system (Delsys, MA, USA) at a sampling frequency of 1200 Hz. GRF were recorded with an in-ground force plate (Advanced Medical Technologies Inc., MA, USA) at a sampling frequency of 1200 Hz.

Data processing

The position and GRF data were both lowpass-filtered with Butterworth filter at a cutoff frequency of 12 Hz. Muscle activation data were bandpass-filtered with Butterworth filters at cutoff frequencies of 20 and 450 Hz. The filtered muscle activation data were further smoothed with an additional lowpass Butterworth filter at a cutoff frequency of 10 Hz. The amplitudes of the smoothed muscle activation data were normalized by the maximum activation of each signal and time-normalized (0 to 100 %) to the duration of the stance phase of the cutting task.

The analysis consisted of a standard OpenSim processing pipeline (Figure 3. 1) (Delp et al., 2007). A musculoskeletal model with 23 degree-of-freedom and 92 muscle actuators

was scaled to the static trial of each subject (Delp et al., 1990). The scaling process created a subject-specific model for each participant based on their respective anthropometrics (e.g., segment lengths) (Figure 3. 1. A). The maximum isometric muscle forces within the generic model were initially scaled via generic (C) and subject-specific (S) multipliers that were based on each participant's estimated muscle volume, which in turn were based on their respective body mass and height (Equation 1, 2, and 3) (Handsfield et al., 2014).

$$F_{Subject}^{MaxIso} = F_{Generic}^{MaxIso} \times (C \times S) \text{ (Equation 1)}$$

$$S = \frac{MuscleVolume_{Subject}}{MuscleVolume_{Model}} \text{ (Equation 2)}$$

$$MuscleVolume = (47 \times Body\ Mass \times Body\ Height) + 1285 \text{ (Equation 3)}$$

The inverse kinematics (IK) tool was used to calculate the joint angles by minimizing differences between virtual model markers and experimental subject markers (Figure 3. 1. B). Static optimization (SO) was used to estimate muscle forces and activations by minimizing the sum of squared activations of each muscle (Figure 3. 1. C). The three-dimensional ankle joint contact forces were computed with the joint reaction analysis tool (Figure 3. 1. E), which used the subject-specific model, IK kinematics, SO-based muscle forces, and GRF data (Steele, Demers, Schwartz, & Delp, 2012). The joint reaction analysis tool was used to calculate the contribution of individual ankle muscles and GRF to the three-dimensional ankle joint contact forces (Figure 3. 1. F) (Maniar, Schache, Sritharan, & Opar, 2018). Given the absence of maximum voluntary isometric contractions, the simulated muscle activations were validated against the processed experimental EMG data through visual inspection and comparison of the muscle

activation patterns (Figure 3. 1. D and Figure 3. 2) (Hamner et al., 2010; Hicks et al., 2015).

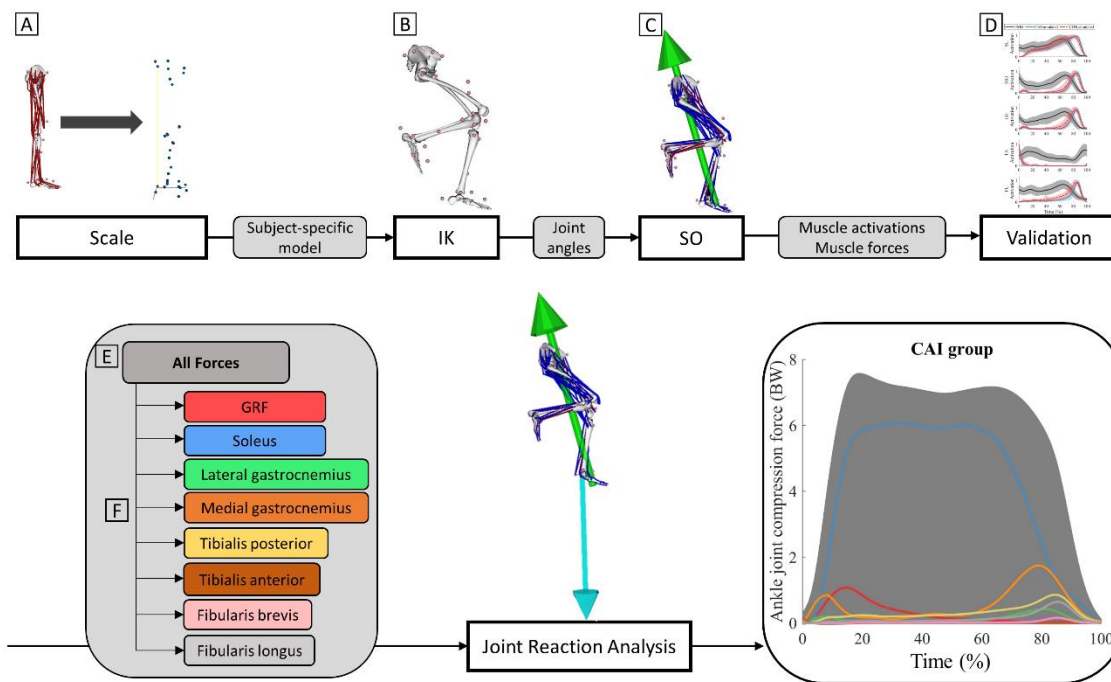


Figure 3. 1 Workflow. A: scaling of model. B: inverse kinematics (IK). C: static optimization (SO). D: validation by comparing pattern of measured muscle activation and simulated activation. E: joint reaction analysis with all forces (e.g., ground reaction force (GRF) and individual muscle). F: separate joint reaction analysis for each force (e.g., GRF or individual muscle)

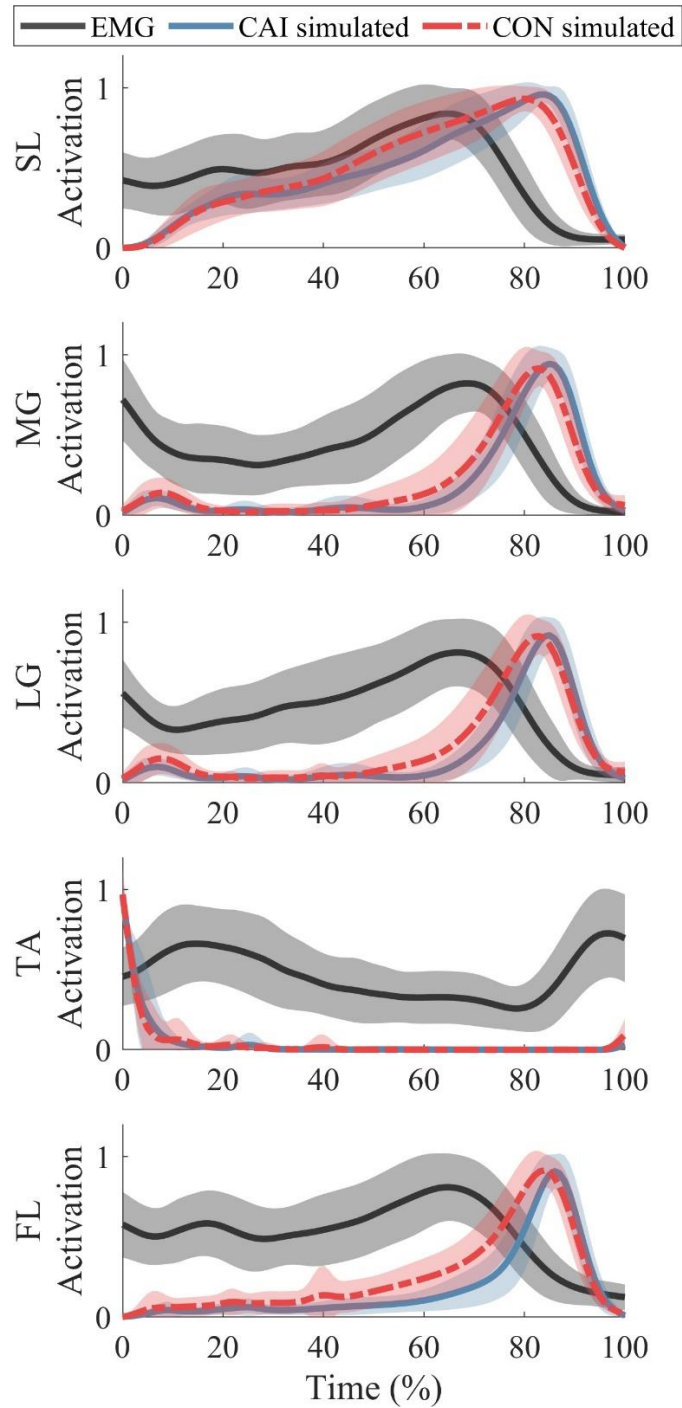


Figure 3. 2 Mean \pm SD normalized muscle activations from EMG and simulation in people with chronic ankle instability (CAI) and healthy controls (CON) during unanticipated cutting. SL: soleus, MG: medial gastrocnemius, LG: lateral gastrocnemius, TA: tibialis anterior, FL: fibularis longus.

Statistical testing

The independent variable for the statistical analysis was group (CAI vs CON). The dependent variables for the statistical analysis were ankle joint (i.e., talocrural joint) compression and anteroposterior shear forces and the contributions of individual muscles and GRF. The normality of all dependent variables was assessed with the Kolmogorov–Smirnov test (Öner & Deveci Kocakoç, 2017). Independent t-tests were used to compare dependent variables between the CAI and CON groups. The alpha level was set at 0.05. Effect sizes (Cohen's *d*) were also calculated for each comparison. Cohen's *d* was considered small if between 0.2-0.5, medium if between 0.5-0.8, and large if greater than 0.8 (J. Cohen, 2013). All statistical analyses were performed in MATLAB (MathWorks, MA, USA).

RESULTS

The independent t-test showed that there was no significant difference between the CAI and CON groups in peak compression force during unanticipated cutting (Figure 3. 3). Furthermore, there were no significant differences between CAI and CON groups in the contributions of individual muscles or GRF to peak ankle joint compression force (Figure 3. 5).

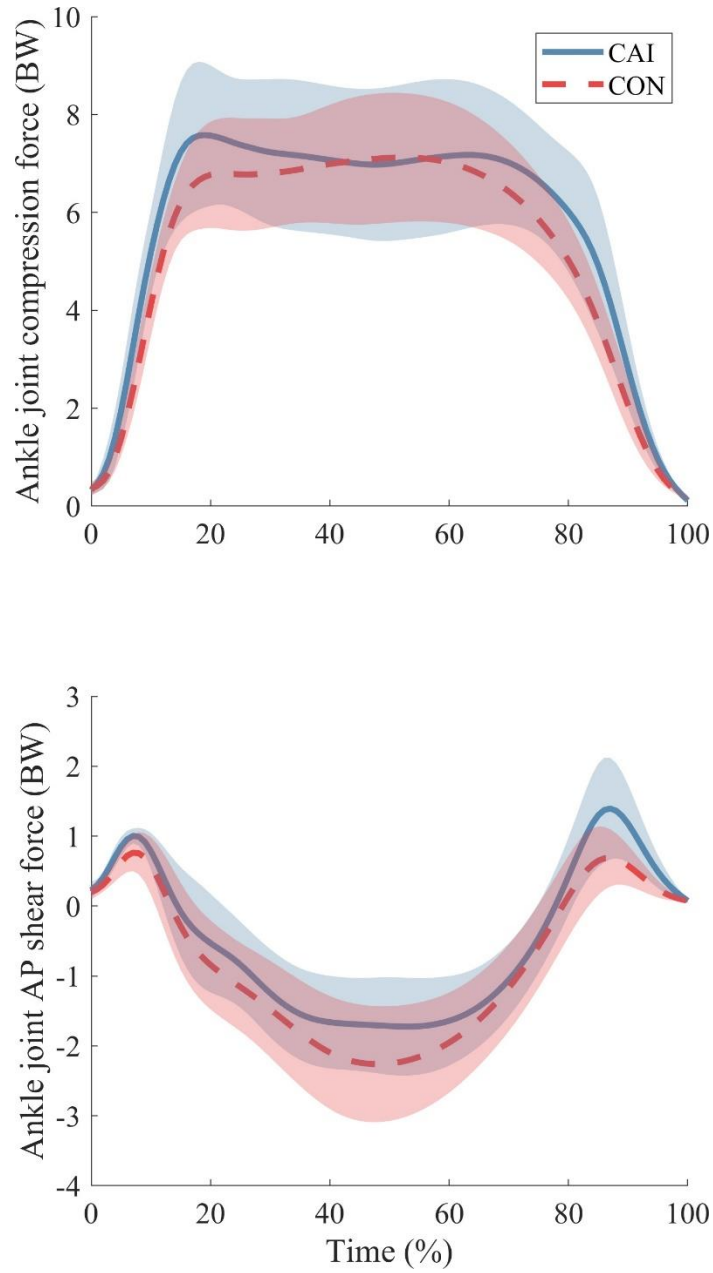


Figure 3. 3 Mean \pm SD normalized time-series ankle joint compression force (top) and anteroposterior shear force (bottom) in people with chronic ankle instability (CAI) and healthy controls (CON) during unanticipated cutting.

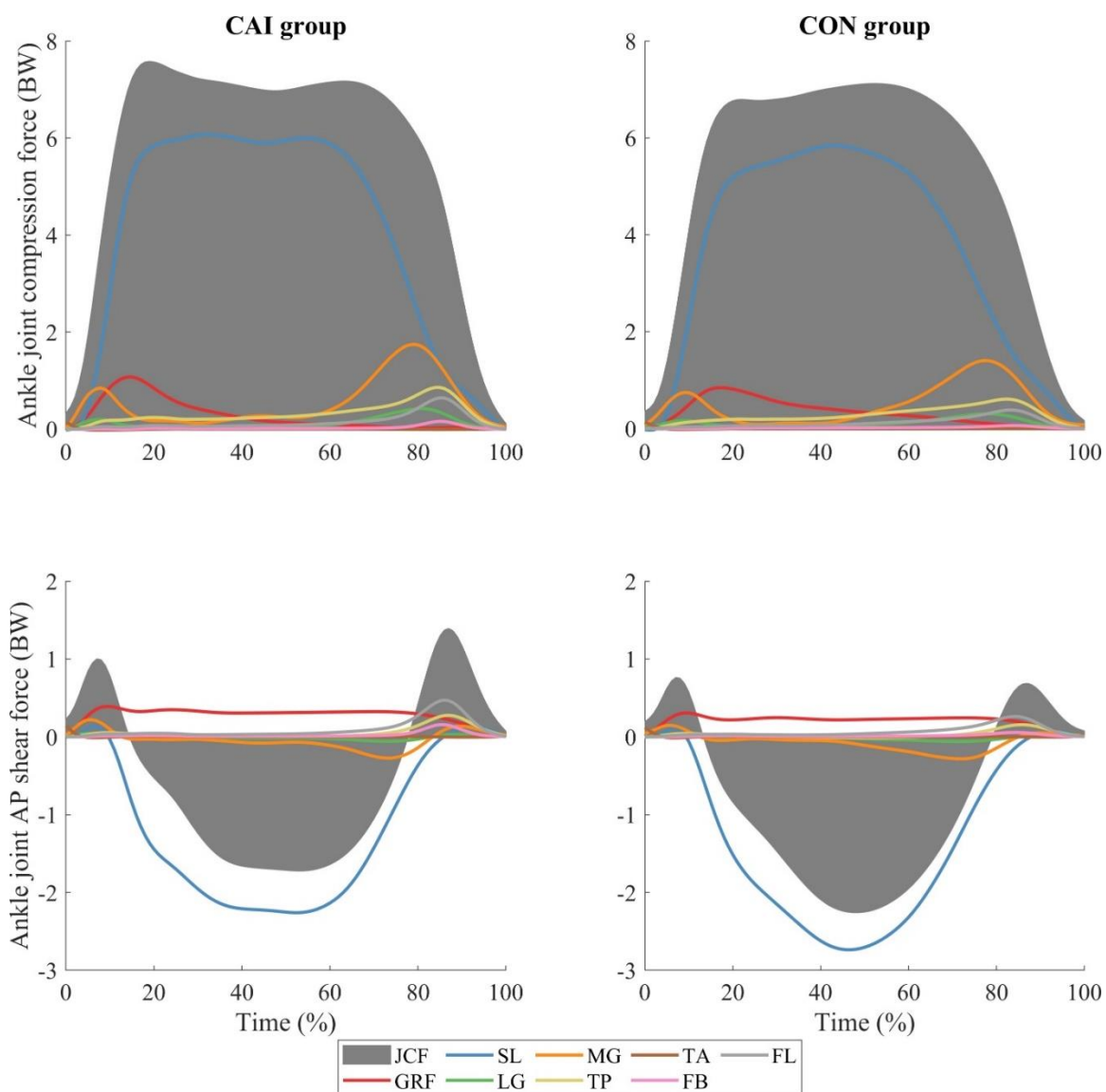


Figure 3. 4 Averaged and normalized ankle joint compression (top row) and anteroposterior (bottom row) forces and contributions from ground reaction forces and individual muscles in people with chronic ankle instability (CAI) and healthy controls (CON) during anticipated cutting. JCF: joint contact force, GRF: ground reaction force, SL: soleus, MG: medial gastrocnemius, LG: lateral gastrocnemius, TP: tibialis posterior, TA: tibialis anterior, FB: fibularis brevis, FL: fibularis longus

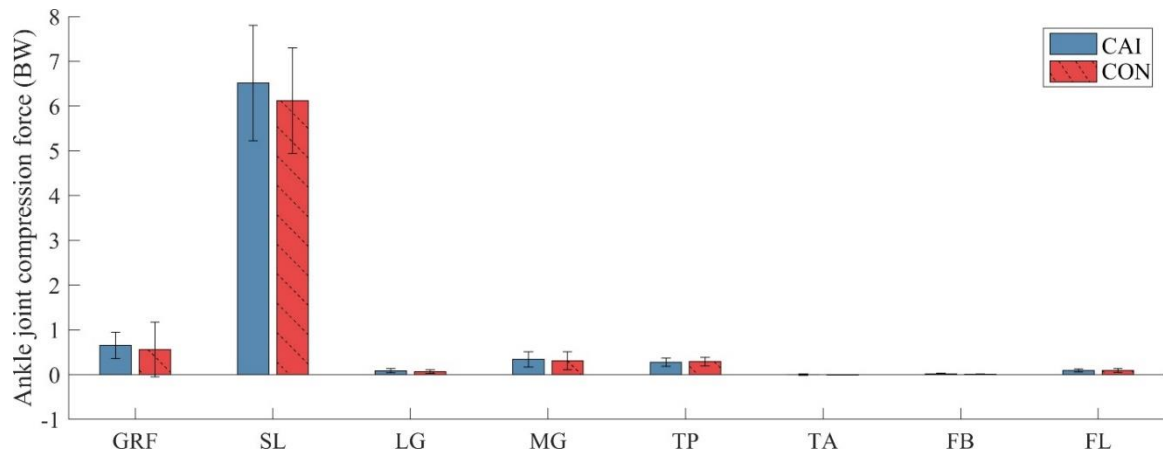


Figure 3. 5 Mean \pm SD normalized contribution of ground reaction force and individual muscles at time of peak ankle joint compression force in people with chronic ankle instability (CAI) and healthy controls (CON) during unanticipated cutting. JCF: joint contact force, GRF: ground reaction force, SL: soleus, MG: medial gastrocnemius, LG: lateral gastrocnemius, TP: tibialis posterior, TA: tibialis anterior, FB: fibularis brevis, FL: fibularis longus

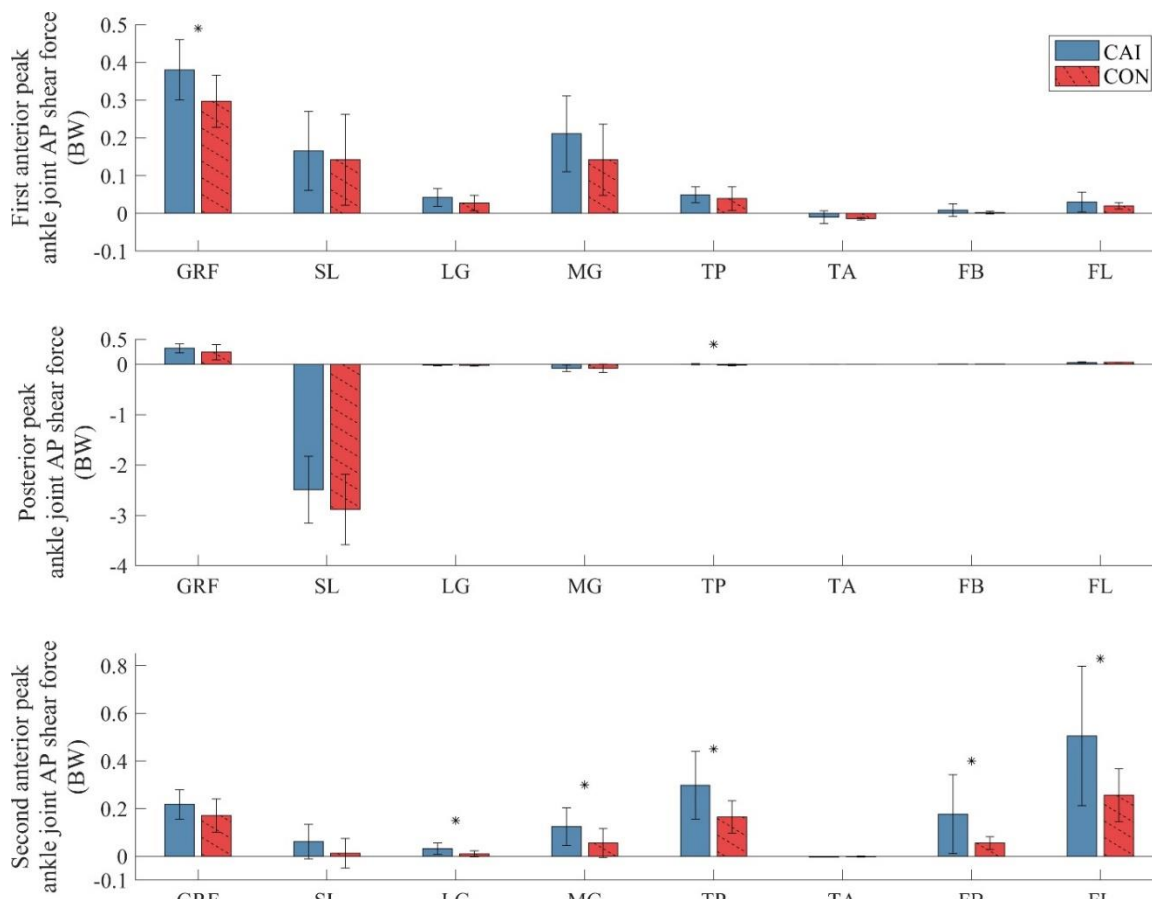


Figure 3. 6 Mean±SD normalized contribution of ground reaction force and individual muscles at time of first anterior, posterior, and second anterior peaks of ankle joint anteroposterior (AP) shear force in people with chronic ankle instability (CAI) and healthy controls (CON) during unanticipated cutting. JCF: joint contact force, GRF: ground reaction force, SL: soleus, MG: medial gastrocnemius, LG: lateral gastrocnemius, TP: tibialis posterior, TA: tibialis anterior, FB: fibularis brevis, FL: fibularis longus, *: significant difference with $p < 0.05$

The independent t-tests showed that there were significant differences between the CAI and CON groups for the first ($p = 0.048$, Cohen's $d = 0.98$) and third ($p = 0.017$, Cohen's $d = 1.21$) peaks in anteroposterior shear forces during unanticipated cutting (Figure 3. 3). Specifically, the two peaks in anterior shear forces in the CAI group were approximately 30% and 92% greater in the CON group.

The contribution of individual muscles and GRF to the first and second peaks in anterior shear forces were also significantly different between the CAI and CON groups (Figure 3. 6). Specifically, people with CAI exhibited greater contribution from the GRF to the first peak in anterior shear force ($p = 0.026$, Cohen's $d = 1.12$) (Figure 3. 6). Furthermore, people with CAI exhibited greater contributions from the lateral gastrocnemius ($p = 0.026$, Cohen's $d = 1.12$), medial gastrocnemius ($p = 0.048$, Cohen's $d = 0.98$), tibialis posterior ($p = 0.017$, Cohen's $d = 1.22$), fibularis brevis ($p = 0.035$, Cohen's $d = 1.05$), and fibularis longus ($p = 0.023$, Cohen's $d = 1.15$) to the second peak in anterior shear force (Figure 3. 6).

DISCUSSION

The purpose of this study was to investigate the contributions from muscle forces and GRF to ankle joint compression and anteroposterior shear forces in people with and without CAI during a cutting task. We found that people with CAI exhibited the greater peaks of ankle joint anterior shear, but not compression forces than the CON group. In addition, people with CAI exhibited greater contribution from GRF to the first peak in ankle joint anterior shear force during early stance, and exhibited greater contribution from lower leg muscles to the second peak in ankle joint anterior shear force during late stance. Together, these results partially supported our hypotheses in that some ankle joint contact forces were greater in people with CAI, and in that these differences were the result of different stance phase specific contributions from individual muscles and GRF.

A primary finding of the current study was that people with CAI exhibited greater ankle joint anterior shear forces during unanticipated cutting compared to people in a CON

group. The observed significance in the differences in anterior shear forces were also associated with a large effect size, which suggests that the differences are both significant and clinically meaningful. This finding is important because previous studies indicated that ankle joint shear forces are strongly associated with the progression of ankle osteoarthritis (N. P. Cohen, Foster, & Mow, 1998; Lane Smith et al., 2000). Interestingly, findings from the current study suggest that the differences in anterior shear forces are the result of stance-phase specific muscle and GRF contributions. Specifically, people with CAI exhibited greater GRF contribution to the first peak in anterior ankle joint shear force compared to people in CON group. The first peak in anterior shear force occurred immediately after foot touchdown during the early stance phase of the cutting task. This phase is also associated with an impact transient in the GRF, which may contribute to the first peak in anterior shear force as the tibia pushes forward against a relatively fixed talus during the landing phase of the cutting task. Previous studies suggest that people with CAI land with protective movement strategies that are characterized by stiffening the ankle joint and adopting a more close-packed ankle position (Son et al., 2017), which could arguably lead to greater peaks in anterior shear force during the early stance phase of cutting. Consequently, this result may indicate that the arthrokinematics and protective movement strategies in people with CAI are partially responsible for the greater peak anterior ankle joint shear forces during at the early stance phase of unanticipated cutting.

Another important finding relates to the group differences in phase-specific contributions by individual muscles to the anterior ankle joint shear forces in people with CAI. Specifically, several muscles exhibited significant differences between-group differences with large effect sizes at the time of the second peak in anterior ankle joint

shear force. This result supports our initial hypothesis and suggests that the greater observed peak in anterior shear force at the ankle joint in people with CAI is the results of different muscle contributions. Greater anterior shear force contributions were observed in some of the plantar flexor (lateral gastrocnemius, medial gastrocnemius, and tibialis posterior) and evtor (fibularis brevis and fibularis longus) muscles during the late stance phase of unanticipated cutting in people with CAI. Notably, the fibularis longus and brevis as well as the tibialis posterior appeared to be the largest contributors to the anterior shear force at the ankle and exhibited the greatest differences in force contributions between the CAI and CON groups. Given that the fibularis longus and brevis are often implicated within the etiology and impairments associated with CAI these findings are perhaps not surprising (Donnelly, Donovan, Hart, & Hertel, 2017; McLeod, Gribble, & Pietrosimone, 2015), but uniquely underscore the importance of restoring appropriate ankle joint function from a mechanical and clinical perspective because these results provide direct links between aberrant ankle joint shear forces and muscle actions. Researchers and clinicians should thus try to establish if restoring fibularis longus function normalizes anterior shear forces and helps mitigate the progression of ankle osteoarthritis in people with CAI.

There are some limitations associated with the methods and results of this study. First, the musculoskeletal model used in the current study does not account for the gliding-sliding joint kinematics of the talocrural joint, including more degrees-of-freedom into the musculoskeletal model may produce more realistic ankle joint kinematics and reveal additional details about joint loads and contributions from muscles. Second, only lower leg muscles were included in the estimating of the muscular contributions to ankle joint contact forces. Given that muscles that do not span a joint can still contribute to the contact force

at that joint (Maniar et al., 2018), including and estimating the effects from other (more proximal) muscles (e.g., quadriceps or gluteus maximus) may provide more additional information for clinicians about which muscles may serve as targets during rehabilitation protocols. Third, the ankle joint shear forces in the mediolateral direction were not considered in the current study. Although mediolateral shear forces in the joint may also damage the joint articular tissue (N. P. Cohen et al., 1998), the magnitudes of the mediolateral shear forces in the current study were much smaller (e.g., peak mediolateral shear force was approximately 25% of peak anteroposterior shear force.) than the joint contact forces in the other two directions, which led us to not disregard them in the current context. Lastly, the results of the current study are based on a sample of 22 people, which could be considered a relatively small sample. Given the general need for replication and extension of research into the areas mentioned above, future studies may thus also consider recruiting larger samples of people with CAI. Additional considerations and directions for future research also relate to the development and use of more detailed and subject-specific models based on a patient's ankle joint morphology with e.g., X-ray or fluoroscopy. Second, the unanticipated cutting task that was chosen for this investigation is an example of a common high-intensity sport task. However, investigating joint contact forces and the specific muscle and GRF contributions during activities of daily living (e.g., walking) may also provide additional insights about how to ameliorate deleterious joint loading and mitigate the progression of ankle osteoarthritis in people with CAI in the long term (Lenton et al., 2018).

CONCLUSION

This study compared joint contact forces and the respective contribution of individual muscles and GRF between people with and without CAI. People with CAI exhibited greater anterior shear forces in the ankle during the early and late stance phases than people without CAI. Furthermore, the greater anterior shear forces were the result of greater GRF contribution during the early stance phase and greater muscle contribution during the late stance phase. It is suggested that clinicians and researchers investigate if targeting these stance phase specific contributions provides a way to also decrease anterior shear forces in an effort to eventually prevent ankle osteoarthritis in people with CAI.

CHAPTER 4: TIME-FREQUENCY ANALYSIS OF MUSCLE ACTIVATION PATTERNS IN PEOPLE WITH CHRONIC ANKLE INSTABILITY DURING LANDING AND CUTTING TASKS

INTRODUCTION

Ankle sprains are among the most common injuries in athletes and physically active people (M. M. Herzog, Kerr, Marshall, & Wikstrom, 2019). Up to 70% of the general population has experienced at least one ankle sprain (McKay, Goldie, Payne, & Oakes, 2001). A previous study also reported that up to 74% of people with a history of ankle sprains develop chronic ankle instability (CAI), which is a condition characterized by recurring or repeated giving away of the ankle during dynamic activities (Gribble et al., 2014; M. M. Herzog et al., 2019). Recurrent ankle sprains are associated with mechanical and functional deficits and become a critical issue in people with CAI because it limits their physical activities (Hubbard & Wikstrom, 2010), and leads to residual symptoms such as pain, swelling, or feeling of giving away (Hertel, 2002). In addition, CAI is associated with the development of ankle osteoarthritis due to damage of the talocrural joint surface (Hintermann et al., 2002; Wikstrom et al., 2013). Furthermore, people with CAI exhibit different neuromuscular strategies, such as altered muscle activations, as they walk or perform sport-related landing or cutting motions (Kim et al., 2019; Son, Kim, Seeley, & Hopkins, 2019).

Electromyography (EMG) is an important research tool to investigate the neuromuscular strategies during sport-related motions, and several studies have used EMG to identify altered neuromuscular strategies of people with CAI compared to people without CAI. (Feger et al., 2015; Herb, Grossman, Feger, Donovan, & Hertel, 2018;

Hertel & Corbett, 2019; Kim et al., 2019; Kunugi et al., 2018; Son et al., 2017). Previous studies revealed different muscle activation strategies during dynamic tasks, such as landing or cutting, in people with CAI compared to healthy people. For example, in some studies people with CAI exhibit less activation of the fibularis longus, tibialis anterior, medial gastrocnemius, and gluteus medius during a jump land and cut task (Son et al., 2017) and diagonal single-leg rebound jumping (Kunugi et al., 2018) compared to healthy controls in previous studies. In contrast, a different study showed that people with CAI muscles exhibit greater activation of the medial gastrocnemius, fibularis longus, adductor longus, vastus lateralis, gluteus medius, and gluteus maximus compared to healthy controls, but only during specific time periods of a jump land and cut task (Kim et al., 2019). Furthermore, fibularis longus, rectus femoris, tibialis anterior, and soleus muscle activations after initial contact did not differ between people with and without CAI during single leg drop jumps (Delahunt, Monaghan, & Caulfield, 2006b). Since results from previous studies show inconsistent findings in the amplitude of muscle activation during dynamic movements, it is possible that investigating and comparing only the amplitudes of muscle activation of people with and without CAI may not provide adequate insight into neuromuscular deficits.

EMG data in studies that investigate neuromuscular control in people with CAI are frequently filtered and smoothed (e.g., band-pass filtered with cutoff frequencies of 20 and 450 Hz and smoothed with root mean square algorithms), which removes, and essentially ignores, information about the frequency domain of EMG data and the neuromuscular recruitment strategies of different muscles (Wakeling et al., 2006). Some studies have investigated the time-frequency domain of EMG data in order to

differentiate between people with different impairments or knee injury history (Jewell, Hamill, von Tscharner, & Boyer, 2019; Kuntze, von Tscharner, Hutchison, & Ronsky, 2015; Mohr, von Tscharner, Emery, & Nigg, 2019; von Tscharner, 2000; von Tscharner & Valderrabano, 2010). For example, von Tscharner and Valderrabano (2010) successfully used time-frequency features of muscle activations to accurately classify people with ankle osteoarthritis and healthy people (von Tscharner & Valderrabano, 2010). However, no study to date has investigated muscle activation characteristics in the time-frequency domain of people with CAI. Given that investigating muscle activation in the time-frequency domain may reveal information about motor unit and muscle recruitment strategies, which are relevant to designing targeted clinical interventions, studying the characteristics of clinically important muscles (e.g., fibularis longus) in this domain in people with CAI seems warranted.

To better understand the neuromuscular strategies used by people with CAI it would be important to investigate the muscle activation patterns in the time-frequency domain. Therefore, the purpose of the current study was to identify differences the time-frequency domain of muscle activation patterns between people with and without CAI during athletic tasks (e.g., landing, anticipated cutting, and unanticipated cutting). We hypothesized that 1) there would be significant differences in the frequencies of muscle activation patterns between people with and without CAI and 2) that these differences would be task-dependent.

METHODS

Participants

Eleven people with CAI (22.4 ± 3.2 years, 1.68 ± 0.11 m, 69.0 ± 19.1 kg) and 11 healthy people (22.6 ± 4.2 years, 1.74 ± 0.11 m, 66.8 ± 15.5 kg) were recruited for this study. All participants signed an informed consent form that was approved by an Institutional Review Board, which ensured that the research complied with the ethical principles of the Declaration of Helsinki. Inclusion criteria for the CAI group were based on a modified version of the Ankle Instability Instrument, which used nine questions to assess various aspects of a person's history of ankle sprains and associated symptoms (Docherty, Gansneder, Arnold, & Hurwitz, 2006; McVey et al., 2005). The Foot & Ankle Disability Index (FADI) and FADI-Sport (FADI-S) questionnaires were additionally used to quantify the function and disability in the ankle joint (FADI, CAI group: $90.3 \pm 9.4\%$, CON: $100 \pm 0\%$; FADI-S, CAI: $88.6 \pm 9.1\%$, CON: $100 \pm 0\%$) (Houston, Hoch, & Hoch, 2015; Kipp & Palmieri-Smith, 2013). Participants from the control group were matched to the CAI group based on sex, age, height, weight, and physical activity level, which was assessed via Tegner scores (Kipp & Palmieri-Smith, 2013).

Data collection

Participants were instrumented with five electromyographical (EMG) sensors (Bagnoli 8-Channel Desktop System, Delsys, Boston, MA, USA). These EMG sensors were attached over the muscle bellies of the lateral gastrocnemius (LG), medial gastrocnemius (MG), fibularis longus (FL), soleus (SL), and tibialis anterior (TA) after cleaning of skin with an alcohol swab on the EMG attached area. Each participant performed three tasks: 1) double-leg forward jump with single-leg landing, 2) double-leg forward jump with single-leg landing and anticipated cutting, and 3) double-leg forward jumping with single-leg landing and unanticipated cutting. The order of the three tasks

remained the same for each participant so that the difficulty increased progressively (e.g., landing, anticipated cutting, unanticipated cutting). For each task, participants were asked to perform the double-leg forward-jump over a 15cm box and to land on a force plate (AMTI OR6, Advanced Medical Technology Inc., Watertown, MA, USA). The distance between initial position and the force plate was each participant's leg length which was measured from anterior superior iliac spine and medial malleolus. For the single-leg landing task, participants were asked to land and stabilize their body for 5 seconds. For the single-leg landing and anticipated cutting task, participants were asked to perform a 90° cut away from their landing leg immediately after landing on the force plate. The single-leg landing and unanticipated cutting task were similar to the anticipated cutting task, but the landing leg and the cutting direction were presented to participants by a visual stimulus that was displayed on a laptop monitor, which was positioned at waist height just behind the force plate, and came on as participants broke a light beam set halfway between the take-off and landing area. Participants were asked to perform between three to five successful trials of each task. Trials were considered successful if participants performed the task according to instructions and landed with their foot entirely on the force plate.

Data processing

Force plate and EMG data were recorded during the stance phase of each task at 1200 Hz. EMG data were amplified by a factor of 1000. The beginning of stance phase was defined as the point when the vertical ground reaction force (GRF) data exceeded 10 N. The end of the stance phase for the single-leg landing was defined as 200ms after the beginning of stance phase, whereas for both cutting tasks it was defined as the point when

the GRF fell below 10 N. We excluded one subject in the control group because of technical problems with the GRF. In addition, two participants in the CAI group were not able to perform the unanticipated cutting task. Therefore, the total number of trials included in the analysis was 183 i.e., 15 less (one CON: 3 tasks x 3 trials; two CAI: 1 task x 3 trials) than if the data set had been complete and included all 198 trials (22 subjects \times 3 tasks \times 3 trials).

Wavelet transformations allow for the simultaneous analysis of EMG signals in the time and frequency domains with various resolutions (von Tscharner, 2000). The intensity of the EMG signal was calculated with a wavelet intensity analysis in which EMG data was transformed in the time-frequency domain with a set of 11 nonlinearly scaled Cauchy wavelets (w1-w11) (Jewell et al., 2019; von Tscharner, 2000). The center frequencies of the wavelets were 6.90, 19.29, 37.71, 62.09, 92.36, 128.48, 170.39, 218.08, 271.50, 330.63, and 395.46 Hz to capture the full range of the EMG signal spectrum (von Tscharner, 2000). The intensities were time-normalized to make 0-100% of stance phase (Figure 4. 1). The intensity from w1 was excluded for further analyses because it was considered to reflect movement artifacts (Conforto, D'Alessio, & Pignatelli, 1999). The total intensities of each wavelet (w2-w11) were compiled into a matrix. The matrix had 915 rows representing (183 trials \times 5 muscles) and 10 columns representing total intensity from w2-w11. A principal component analysis was applied to the matrix to find the principal components (PC) that accounted for 90% of the total variance (VAF).

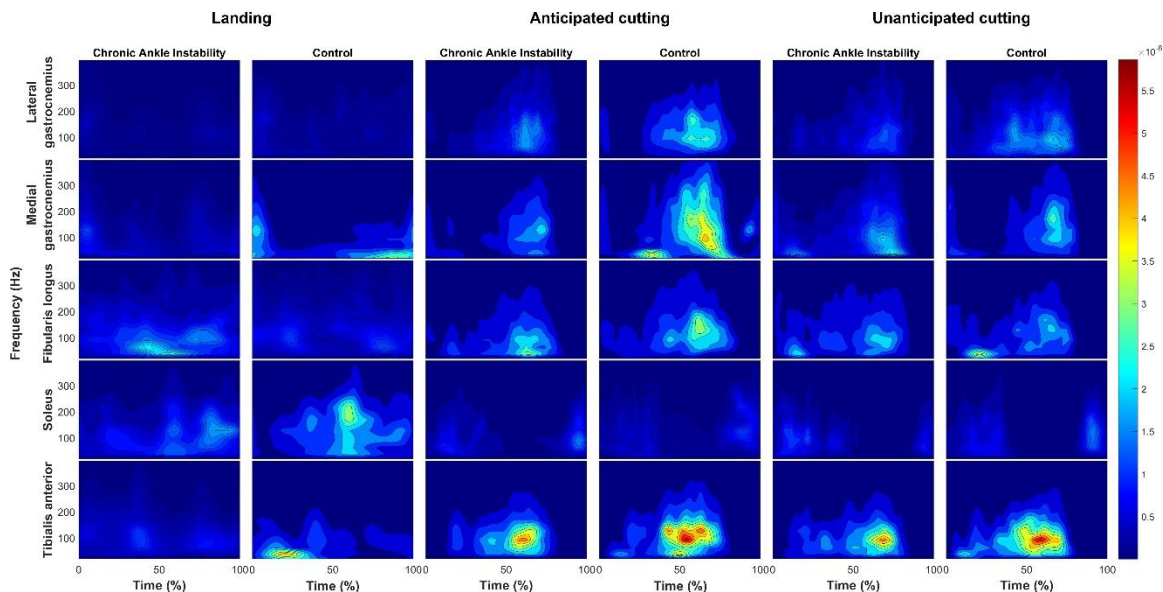


Figure 4. 1 Time-frequency heatmaps for mean wavelet intensities of the lateral gastrocnemius (first row), medial gastrocnemius (second row), fibularis longus (third row), soleus (fourth row), and tibialis anterior (fifth row) during 200 ms of the landing task (left two columns) and during the stance phases of the anticipated cutting task (middle two columns) and unanticipated cutting task (right two columns).

Statistical analysis

For the statistical analysis, the dependent variables were the extracted PC scores. The independent variables were group (CON and CAI), task (landing, anticipated cutting, and unanticipated cutting), and muscles (SL, FL, TA, MG, and LG). The Kolmogorov-Smirnov test was used to check the normal distribution of the PC scores. Separate three-way ANOVAs for each PC Score were used to analyze the interactions and main effects of all experimental conditions. Fisher's Least Significant Difference procedure was used during post hoc testing to investigate pair-wise differences for any significant interactions or main effects. Two-way interactions not involving group as a factor and main effects other than group were not investigated because they did not directly relate to the purpose

of the study (e.g., task \times muscle differences were not of interest). Alpha value was set to 0.05.

RESULTS

The PCA extracted two PCs, which accounted for 71% and 18% of the total variance in the EMG input data (Figure 2). The first PC captured variation in the magnitude of the wavelet intensities whereas the second PC captured variation related to a shift in the center frequencies of wavelet intensity.

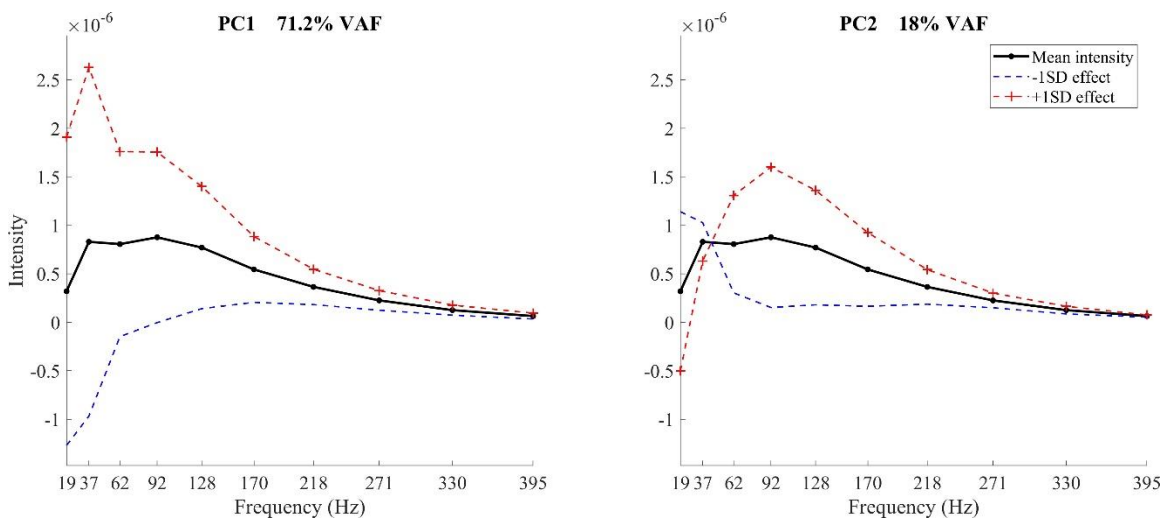


Figure 4. 2 Variation in wavelet intensity captured by the two principal components (PC). The effects of positive and negative PC scores on wavelet intensities are illustrated by simulating a one standard deviation (1SD) change in the PC on the mean intensity of the EMG data and can be visualized by the dashed lines and the + and – symbols, respectively. The effects. VAF – variance accounted for by the given PC.

None of the three-way interactions between group, task, and muscle were significant for either PC (Table 1). In addition, neither of the two-way interactions that included Group as a factor were significant for the first PC. There was, however, a

significant ($p = 0.041$) two-way interaction between Group and Task for the second PC (Figure 3). Post hoc testing revealed that the scores of PC2 were significantly ($p = 0.009$) lower in all muscles of the CAI group during the anticipated cutting task only. Lastly, there was also a significant ($p = 0.009$) main effect of group for the scores of the first PC, which showed that the CAI group exhibited lower PC1 scores across all tasks and for all muscles (Figure 4).

Table 4. 1 Principal component (PC) scores (means and standard deviation) for lateral gastrocnemius (LG), medial gastrocnemius (MG), fibularis longus (FL), soleus (SOL), and tibialis anterior (TA) in people with chronic ankle instability (CAI) and for healthy controls (CON) for the landing (Land), anticipated cutting (Ant), and unanticipated cutting (Unant) tasks.

Muscle	Group	PC1 score			PC2 score		
		Land	Ant	Unant	Land	Ant	Unant
LG	CAI	-12.60±1.73	-6.48±6.84	-7.16±5.89	-7.72±1.54	-2.11±6.31	-3.08±4.58
	CON	-10.87±2.89	-0.89±12.95	-0.44±11.17	-6.88±2.77	5.14±13.85	1.08±7.85
MG	CAI	-6.65±7.21	-2.34±7.92	0.48±7.90	-5.92±3.82	-1.61±4.12	-1.61±3.19
	CON	10.13±87.45	16.27±77.59	-1.30±7.39	10.06±38.11	2.83±18.50	0.17±6.01
FL	CAI	5.49±34.98	2.62±22.47	2.54±13.36	3.26±14.91	1.30±7.81	3.04±9.33
	CON	-4.68±16.25	1.63±24.68	3.95±22.18	-0.84±13.54	6.67±24.11	0.01±15.66
SOL	CAI	0.69±17.88	-8.18±5.90	-7.97±5.78	2.53±14.53	-4.24±4.68	-3.95±5.35
	CON	7.27±21.97	-9.08±4.86	-7.89±7.54	7.41±17.23	-4.70±5.69	-3.99±6.12
TA	CAI	-5.72±4.29	4.60±8.78	5.74±11.10	-2.27±4.24	7.36±8.33	5.82±8.69
	CON	8.00±48.28	11.31±30.70	13.75±35.19	-7.06±11.43	10.58±19.51	9.82±23.65

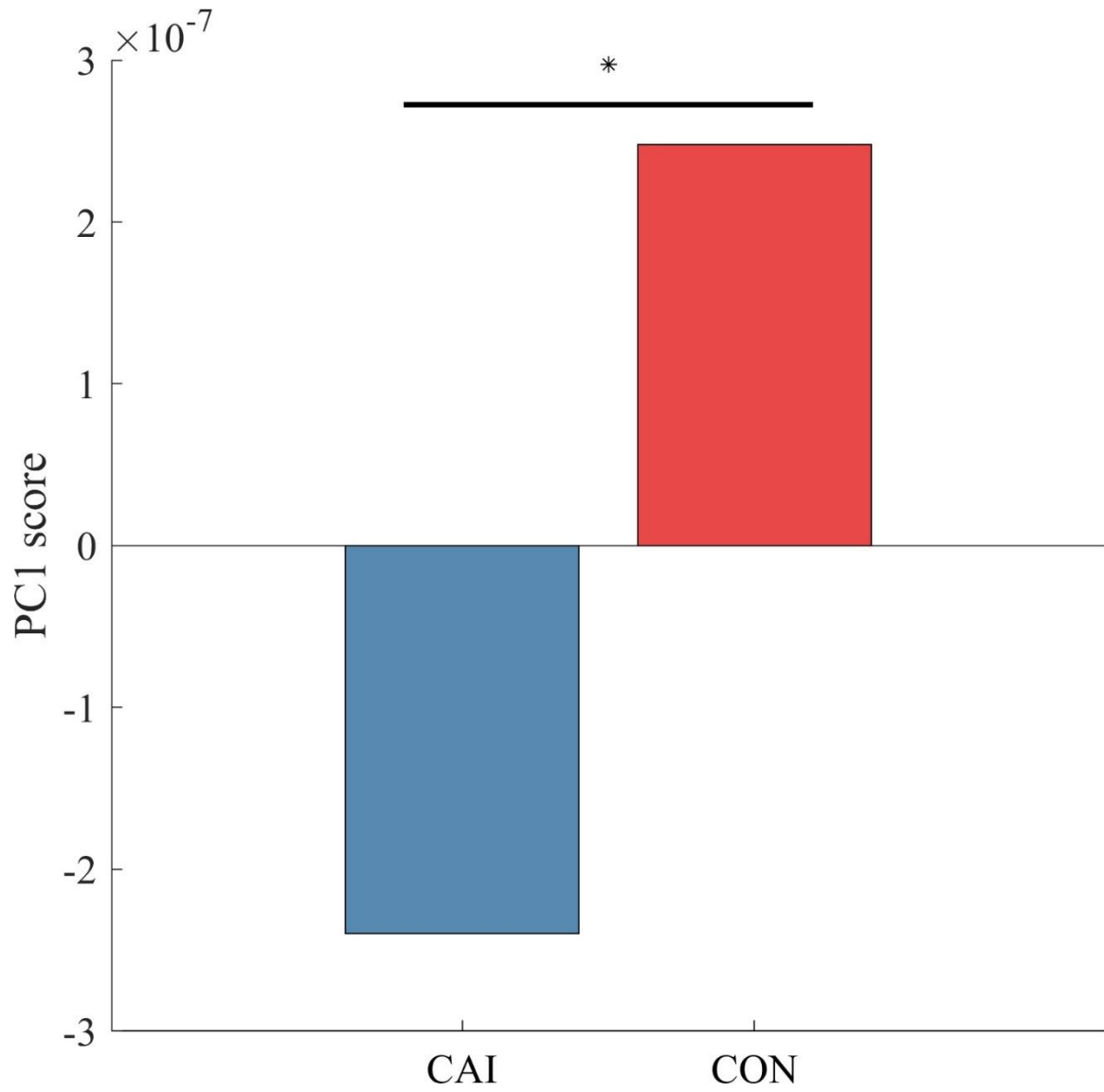


Figure 4. 3 Muscle- and task-averaged PC1 scores (i.e., magnitude of the wavelet intensities) for people with chronic ankle instability (CAI) and for people in the control group (CON)

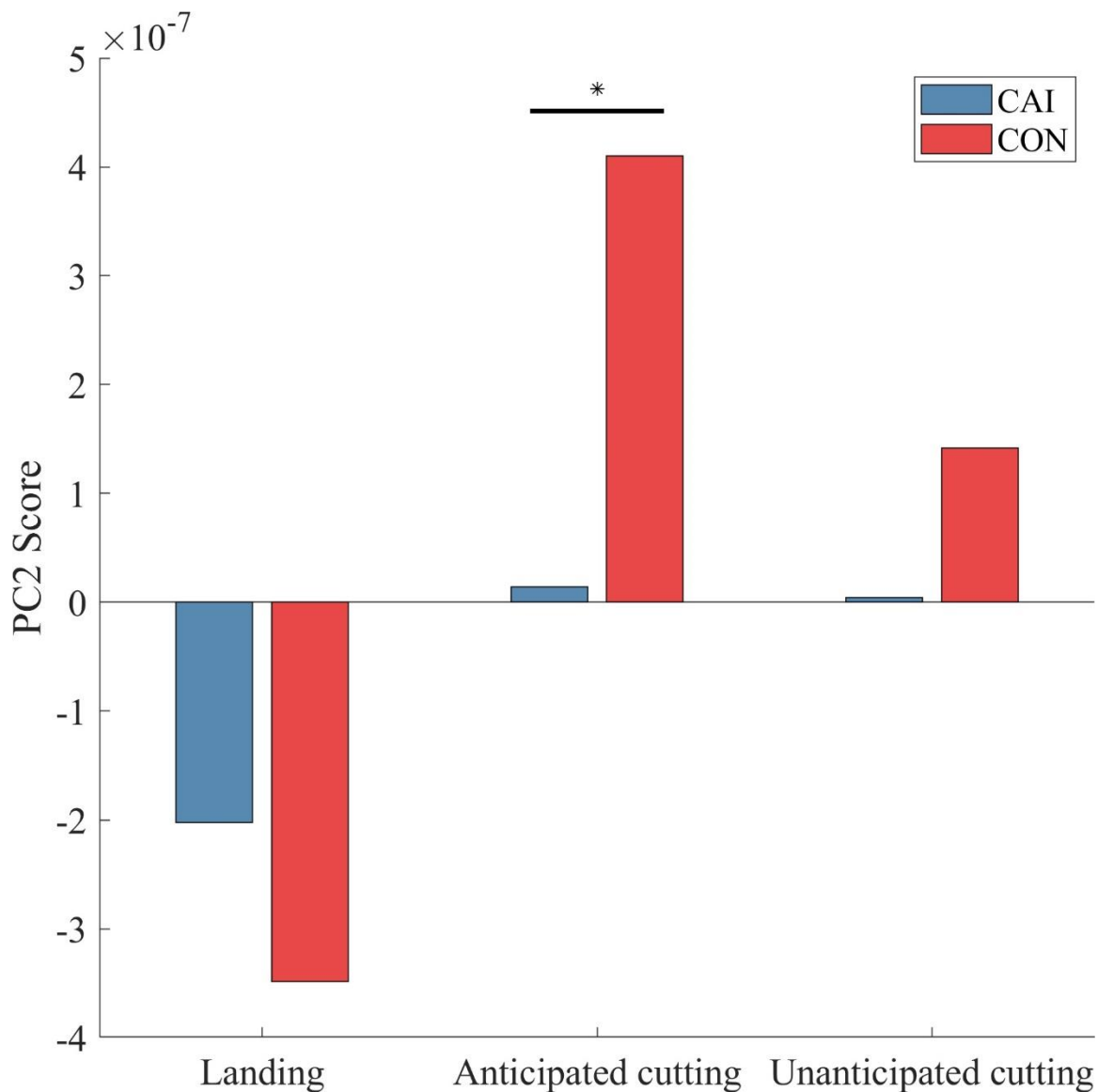


Figure 4. 4 Muscle-averaged PC2 scores (i.e., shift in center frequencies of wavelet intensities) for people with chronic ankle instability (CAI) and for people in the control group (CON) during the landing, anticipated cutting, and unanticipated cutting task.

DISCUSSION

The purpose of the current study was to investigate differences in the time-frequency domain of muscle activation patterns between people with and without CAI during athletic tasks (e.g., landing, anticipated cutting, and unanticipated cutting). We

hypothesized that people with CAI would exhibit different activation patterns and that these differences would depend on the respective task. The results generally supported our hypotheses in that people with CAI exhibited lower wavelet intensities across all muscles and tasks, and were not able to increase wavelet intensities at higher frequency ranges during the anticipated cutting task.

The main effect for PC1 indicated that compared to the CON group, people with CAI exhibited lower PC1 scores in all muscles and across all tasks. Since PC1 captured the general magnitude of wavelet intensities across all frequencies, people with CAI therefore exhibited lower wavelet intensities across all frequency ranges in all muscles and tasks. People with CAI thus appear to use a neuromuscular strategy characterized by activating ankle muscles at lower wavelet intensities during landing and cutting tasks. Previous studies that investigated neuromuscular function in people with CAI during dynamic movements presented inconsistent findings with respect to the peak amplitude of the smoothed EMG signal in that they show that people with CAI exhibit either less activation of the FL, TA, and MG muscles (Son et al., 2017) or more activation of the FL and MG muscles (Kim et al., 2019) than healthy controls. The intensity of a wavelet provides a good approximation of power of the EMG signal at that respective frequency, is related to changes in the Root Mean Square of EMG, and provides insight into the number of active motor units (Jewell et al., 2019; von Tscharner, 2000; von Tscharner & Valderrabano, 2010). The current finding therefore suggests that people with CAI recruit fewer motor units in ankle muscles regardless of task, and is in agreement with research that showed less activation ankle muscles in people with CAI (Son et al., 2017). The current study thus expands on previous results since the wavelet analysis accounts for the intensities across a

wide range of activation frequencies, and presumably motor units (von Tscharnner, 2000). Collectively, these findings suggest CAI rehabilitation may need to include resistance training exercises that aim to increase muscle force production across a large range of activation frequencies so that all motor units are adequately trained. In other words, resistance training exercises should include not only various loads (e.g., heavy vs light loads) but also various speeds (e.g., slow joint movement vs fast joint movement).

The group by task interaction effect for PC2 indicated that people with CAI exhibited similar PC2 scores across all tasks, whereas people in the CON group did not. Specifically, post hoc testing revealed that people in the CON group exhibited greater PC2 scores than the CAI group during the anticipated cutting task. Since PC2 captured a shift among the range of frequencies where the wavelet intensities were most prominent, the increase in PC2 scores in the CON group suggests that this group exhibited an increase in wavelet intensities at higher frequency ranges during the anticipated cutting task. In other words, people with CAI seemed unable to increase wavelet intensities in higher frequency ranges during anticipated cutting. The frequency domain of a muscle's activation profile is influenced by the recruitment of different motor unit types because the conduction velocity of motor units differs based on the electric properties of the motor units i.e., faster motor units exhibit higher conduction velocities and greater wavelet frequencies during muscle activation than slower motor units (Buchthal, Guld, & Rosenfalck, 1955; Wakeling & Syme, 2002). Since cutting motions require rapid muscle activation, these movements also likely require that motor units are recruited at higher frequencies (S. S. Lee, de Boef Miara, Arnold, Biewener, & Wakeling, 2013). Based on the analysis of PC2 scores, it thus appears that people with CAI are not able to recruit motor units during the anticipated cutting task

in the same manner as people in the CON group. This finding may indicate that people with CAI are not able to adequately scale the recruitment of motor units in the frequency domain in response to different task demands. Given that movements are controlled with not only the intensity of muscle activations but also speed of motor unit recruitment, which suggests that people with CAI may stem from incapacity to scale frequency of muscle activations during the dynamic tasks. Perhaps, performing resistance training exercises during CAI rehabilitation at fast velocities may facilitate the recruitment and increase the firing rate of faster motor units and thus improve the capacity to shift wavelet intensity towards higher frequency during muscle activation in people with CAI.

There are several limitations with the current study. First, the FADI and FADI-Sport questionnaires were used to assess self-reported ankle function in the current study. Other studies, however, have used questionnaires such as the Cumberland Ankle Instability Tool (Gribble et al., 2014). Although the Cumberland Ankle Instability Tool is commonly used, FADI and FADI-Sport are considered to adequately describe functional deficits in people with CAI (Houston et al., 2015). In addition to the FADI and FADI-Sport, we also used another questionnaire to evaluate the history and symptoms of ankle sprain (McVey et al., 2005), which enhanced the CAI inclusion criteria. Second, the current study did not include a group of “copers” (i.e., people who have a history of lateral ankle sprain but have no recurrent ankle sprains or functional deficits). A previous study revealed that copers exhibit different sensorimotor function than people with CAI (Wikstrom et al., 2012). For this reason, recruiting a copers group in addition to people with CAI and healthy controls may provide better clinical insights and more detailed information about the spectrum of functional deficits in people with CAI. Third, only the landing and stance phases during

three tasks were analyzed in this study. However, the phase immediately before foot contact can provide information about preparatory strategies during the dynamic tasks and has been widely analyzed in previous CAI studies (Minoonejad, Karimizadeh Ardakani, Rajabi, Wikstrom, & Sharifnezhad, 2019; A. Rosen et al., 2013). Therefore, analyzing muscle activation in the frequency domain during the preparatory phase of dynamic tasks in people with CAI in future studies may also provide additional information. Fourth, we only collected and analyzed EMG of distal muscles (i.e., at the ankle joint). Including proximal muscles for time-frequency analysis in future studies may also be useful because previous research suggests that people with CAI also exhibit different activation patterns of proximal muscles, such as the vastus lateralis and gluteus maximus (Kim et al., 2019). Lastly, the sample size of people with CAI in this study is relatively small, which may suggest that the results and interpretations should be considered as preliminary and should be replicated in a larger sample.

To our knowledge, this study is the first study to investigate the time-frequency domain of muscle activation patterns in people with CAI. There are several clinical implications of the results from the current study. We found that people with CAI exhibited lower wavelet intensities across all tasks and all muscles and did not change the muscle activation in the time-frequency domain in response to different tasks. Collectively, people with CAI appear to activate fewer motor units in all ankle muscles we analyzed during all studied dynamic tasks, and recruit slower motor units within all analyzed ankle muscles during anticipated cutting. Given that people with CAI exhibited neuromuscular deficits in both wavelet intensity and frequency of ankle muscle activations in the current study, rehabilitation to improve neuromuscular control and decrease risk of recurrent injuries in

people with CAI will likely need to include exercises that focus on the velocity component of contraction (e.g., anticipated and unanticipated tasks with various moving directions) in addition to the intensity component (e.g., loads) of contraction.

CONCLUSION

People with CAI exhibited muscle activation patterns characterized by differences in the time-frequency domain compared to healthy people. Specifically, people with CAI activated all ankle muscles with lower wavelet intensities across the entire frequency spectrum, regardless of task. In addition, people with CAI did not exhibit an increase in wavelet intensity in higher ranges of the frequency spectrum during the anticipated cutting task. These findings suggest that rehabilitation efforts for people with CAI should consider that this population exhibits differences in neuromuscular control that exist not only in the overall magnitudes, but also in the time-frequency domain, of muscle activation patterns.

CHAPTER 5: MUSCLE SYNERGIES IN PEOPLE WITH CHRONIC ANKLE INSTABILITY DURING ANTICIPATED AND UNANTICIPATED CUTTING TASKS

INTRODUCTION

A sprain of the ligaments that are located on the lateral side of the ankle joint is one of the most common musculoskeletal injuries. Up to 70% of people who sprain their ankles develop chronic ankle instability (CAI) and experience lingering mechanical and functional deficits (Gribble et al., 2016). Although researchers have investigated and developed rehabilitation strategies for people with CAI, three billion health care dollars continue to be spent annually to treat CAI in the United States (Radwan et al., 2016). Furthermore, people with CAI face higher risks of developing more serious clinical sequelae, such as ankle osteoarthritis (Carbone & Rodeo, 2017; Wikstrom et al., 2013).

Researchers have previously investigated neuromuscular function in people with CAI and identified numerous deficits (Hertel & Corbett, 2019). Electromyography has been widely used in these studies and revealed a variety of neuromuscular deficits, such as less muscle activity (Son et al., 2017), delayed activation (Flevas et al., 2017), compensatory control of proximal joints (DeJong et al., 2020; Kim et al., 2019; Rios et al., 2015), or longer duration of activation (Feger et al., 2015) in people with CAI. While these studies primarily described neuromuscular function of the peripheral nervous system, few studies have investigated deficits in neuromuscular control at the level of the central nervous system (CNS) in people with CAI. The CNS, however, plays an important role in controlling muscle activity and joint stiffness and in stabilizing joints during movement (Humphrey & Reed, 1983; Swanik, Covassin, Stearne, & Schatz, 2007). Despite the

importance of these roles, CNS-based control of neuromuscular activation or muscle activation strategies have not been investigated in people with CAI. Although some researchers have investigated, and found evidence for, deficits in CNS function in people with CAI, the methods used by these researchers (e.g., functional near-infrared spectroscopy or transcranial magnetic stimulation) only allow for the study of the CNS during static tasks (e.g., single-limb standing) (Needle et al., 2013; A. B. Rosen et al., 2019). Given that ankle sprains frequently occur during fast and dynamic movements, it is necessary to extend the investigation of CNS control in relation to neuromuscular activation patterns to such movements.

One way to study CNS control of muscle activation patterns or strategies is via the analysis of muscle synergies through the use of non-negative matrix factorization (NMF) (d'Avella et al., 2003; D. D. Lee & Seung, 1999; Rabbi et al., 2020). The analysis of muscle synergies has been used to identify CNS deficits in patients with neurological pathologies, such as stroke or cerebral palsy (Allen et al., 2019; Shuman et al., 2019). This analysis provides meaningful insights about CNS control, such as the complexity of an individual's strategy to control the activations of multiple muscles during movement, which is reflected in the number of muscle synergies that are present during a specific task (Safavynia et al., 2011). People who exhibit a smaller number of muscle synergies appear to use a less complex control strategy, as demonstrated by patients with neurological pathologies who appear to control muscle activations with broader and merged versions of muscle synergies found in healthy people (Safavynia et al., 2011). In addition, the similarity among synergies between people with neurological pathologies and healthy people are used to identify similarities in CNS control signals and impairments in descending neural commands

(Safavynia et al., 2011). Given that CAI is also often considered to affect CNS function similar to other neurological pathologies (Needle et al., 2017; Needle et al., 2013; A. B. Rosen et al., 2019), investigating muscle synergies in people with CAI may provide unique insight into their neuromuscular control strategies during dynamic tasks.

Therefore, the purposes of this study were to use NMF and extract muscle synergies in order to investigate and compare CNS-based neuromuscular control strategies in people with CAI and healthy CON during cutting tasks. We hypothesized that people with CAI would 1) use fewer (i.e., less complex) muscle synergies, 2) exhibit different muscle-specific weightings within muscle synergies, 3) display task-specific these differences in muscle synergies.

METHODS

Participants

Eleven people with CAI (22 ± 3 years, 1.68 ± 0.11 m, 69.0 ± 19.1 kg) and 11 healthy controls (CON) (23 ± 4 years, 1.74 ± 0.11 m, 66.8 ± 15.5 kg) were recruited to participate in the current study. Initial screening and inclusion into the CAI group was based on a questionnaire (McVey et al., 2005). In addition, the foot and ankle disability index (FADI) and FADI-Sport questionnaires were used to assess ankle joint function (Hale & Hertel, 2005), and Tegner scores were used to quantify physical activity level of each participant.

Data collection

Ground reaction forces (GRF) were recorded with a force platform (AMTI, MA, USA) and muscle activations were recorded with a desktop EMG system (Bagnoli,

Delsys, MA, USA). Muscle EMG and GRF data were collected at sampling frequencies of 1200 Hz. Five EMG electrodes were attached on lateral gastrocnemius (LG), medial gastrocnemius (MG), fibularis longus (FL), soleus (SL), and tibialis anterior (TA) muscles. Each participant performed a brief warm-up, after which they were asked to perform up to five trials each of an anticipated and unanticipated cutting task. For both tasks, participants performed a forward jump over a 15 cm box and onto a force plate. The distance between the initial position and the force plate was normalized to each participant's leg length, which was defined as distance between the anterior superior iliac spine and the medial malleolus of the same leg. Participants were asked to land on their involved leg and perform a 90° cut away from their landing leg as quick as possible after landing on the force plate. During the anticipated cutting task (Ant), the direction of the cut was given to each participant before each jump. During the unanticipated cutting task (Unant), the direction of the cut was indicated to each participant via an electronic signal displayed on a computer screen, which was positioned at waist-height in front of the force plate. The signal was triggered once a participant broke a light beam that was projected from a light gate, which was positioned halfway between the initial start position and the force plate. Data from one participant in the CON group had to be excluded because of problems with the GRF data. In addition, two people in the CAI group were not able to perform the unanticipated cutting tasks. The total number of trials included in this study was 9 less than 132 trials (22 subjects \times 2 tasks \times 3 trials).

Data processing

Data were analyzed from the stance phase of each task. The stance phase of the cutting tasks was based on GRF thresholds of 10 N for both touchdown and takeoff. The

EMG data was low-pass filtered with a cutoff frequency of 450 Hz and high-pass filtered with a cutoff frequency of 20 Hz. The filtered EMG data were rectified and smoothed with a low-pass filter at cutoff frequency of 10 Hz. The smoothed activation data for each muscle were normalized to the maximum activation observed during all trials and time-normalized to 101 data points such that 0% represented touchdown and 100% represented takeoff (Figure 5. 1) (Banks, Pai, McGuirk, Fregly, & Patten, 2017). The smoothed and time-normalized muscle activation data from each subject and each task were organized into a 5 by 303 matrix (i.e., 5 rows for all 5 muscles and 303 columns for 3 trials of 101 data points). Each muscle's activation was further divided by its standard deviation to obtain unit variance so that NMF can extract equally weighted muscle synergies (Chvatal & Ting, 2013). NMF was set to extract time-invariant muscle synergy vectors (W) and time-variant muscle activation coefficients (C) from the 5 x 303 EMG matrix based on the following equation (Equation 1) (Chvatal & Ting, 2013).

$$M = \sum_{i=1}^{N_{synergy}} W_i C_i + \varepsilon \quad (\text{Equation 1})$$

The total variance accounted for (VAF_{Total} : Equation 2) and variance accounted for by each muscle (VAF_{Each} : Equation 3) were calculated iteratively with continuously greater number of synergies until the following criteria were met: 1) VAF_{Total} was $\geq 90\%$ and 2) $VAF_{Each} \geq 75\%$ (Chvatal & Ting, 2013). In most data sets, three synergies were the appropriate number of muscle synergies with the criteria. Muscle synergies were sorted based on timing of peak activation coefficient and Cosine-Similarity of synergy vectors (Boccia, Zoppiroli, Bortolan, Schena, & Pellegrini, 2018).

$$VAF_{Total} = 1 - \frac{\sum_{i=1}^p \sum_{j=1}^n (e_{i,j})^2}{\sum_{i=1}^p \sum_{j=1}^n (E_{i,j})^2} \quad (\text{Equation 2})$$

$$VAF_{Each_m} = 1 - \frac{\sum_{j=1}^n (e_{m,j})^2}{\sum_{j=1}^n (E_{m,j})^2} \text{ (Equation 3)}$$

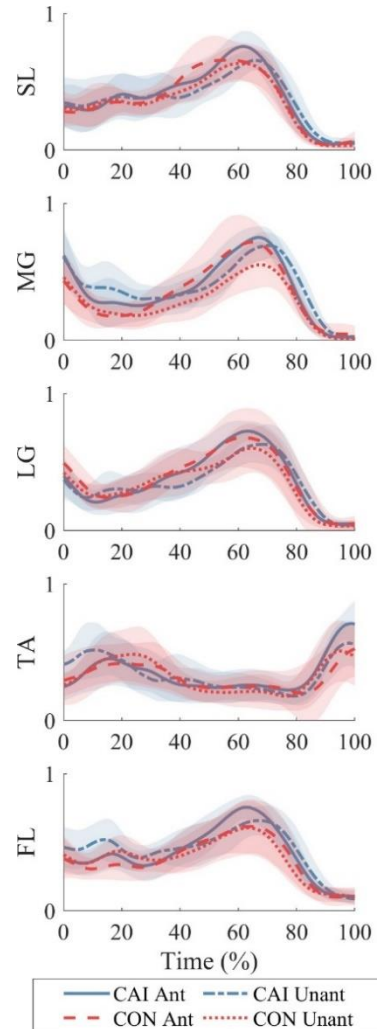


Figure 5. 1 Mean \pm SD normalized muscle activity in people with chronic ankle instability (CAI) and healthy controls (CON) during anticipated (Ant) and unant (Unant) cutting. SL: soleus, MG: medial gastrocnemius, LG: lateral gastrocnemius, TA: tibialis anterior, FL: fibularis longus.

Statistical analysis

The independent variables for the statistical analyses were group (CAI and CON) and task (Ant and Unant). The dependent variables for the statistical analyses were the

number of muscle synergies, the VAF_{Total} of each synergy, and the muscle-specific weightings from each of the extracted synergies. Zero-lag cross-correlation and cosine-similarity values were used to test the similarity of activation coefficients and synergy vectors, respectively, between each group and task for each synergy (i.e., CON Ant vs Unant, CAI Ant vs Unant, CON vs CAI Ant, CON vs CAI Unant). These tests were used to ensure that the extracted time-variant of the original EMG activation profiles components (i.e., activation coefficients) and the time-invariant components of the muscle synergy vectors (i.e., weighting coefficients) were similar between groups and across conditions, and thus appropriate for subsequent analysis and statistical comparisons. Data with cross-correlation and cosine-similarity values greater than 0.80, respectively, were considered to exhibit high similarity (Boccia et al., 2018).

The normality of all dependent variables were checked with the Jarque-Bera test (Öner & Deveci Kocakoç, 2017). A Wilcoxon rank sum test was used to compare the number of synergies between CAI and CON groups separately for each task (Ant and Unant). A two-way analysis of variance (ANOVA) was used to compare the VAF_{Total} between CAI and CON groups across group and task. Separate two-way ANOVAs were used to compare the muscle-specific weightings for each of the extracted synergies.

RESULTS

Based on the VAF results, two to four synergies were determined as the appropriate number of synergies to represent the EMG data of each trial. In most cases, three synergies were sufficient to reconstruct the EMG data (Figure 5. 2) and the average VAF_{Total} for three synergies was approximately 93%. There was no significant difference in the number of

synergies expressed by the CAI and CON groups during either of the tasks. In addition, there were no significant interaction or main effects for VAF_{Total} .

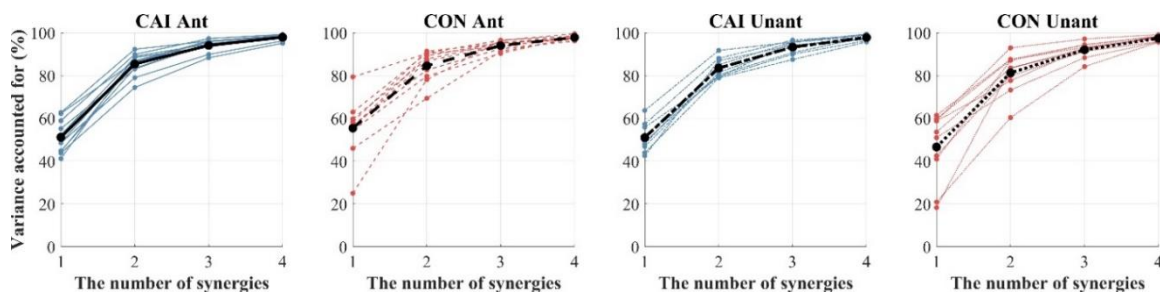


Figure 5. 2 Variance accounted for the synergies for each group during each task (CAI: chronic ankle instability group, CON: healthy control, Ant: anticipated landing-cutting, Unant: unanticipated landing-cutting).

The cosine similarity values for synergy vectors of Synergy 1 and Synergy 2 were greater than 0.80 for all group and task comparisons (Table 5. 1). In contrast, the cosine similarity values for synergy vectors of Synergy 3 were less than 0.8 for all but one group comparison (Table 5. 1). Specifically, the cosine similarity value for the synergy vectors of the CON Unant and CAI Unant comparison was 0.85. The zero-lag cross-correlation coefficients of all activation coefficients from all respective group and task comparisons were greater than 0.80 (Table 5. 2).

Table 5. 1 Cosine-similarity coefficients for each synergy vector comparison (CAI: chronic ankle instability group, CON: healthy control, Ant: anticipated landing-cutting, Unant: unanticipated landing-cutting).

		Synergy #1	Synergy #2	Synergy #3
CON Ant	vs. CON Unant	0.98 ± 0.02	0.82 ± 0.13	0.78 ± 0.17
CON Ant	vs. CAI Ant	0.98 ± 0.02	0.81 ± 0.12	0.72 ± 0.22
CON Unant	vs. CAI Unant	0.98 ± 0.01	0.85 ± 0.10	0.85 ± 0.14
CAI Ant	vs. CAI Unant	0.99 ± 0.01	0.83 ± 0.12	0.78 ± 0.20

Table 5. 2 Zero lag cross-correlation coefficients for each activation coefficient comparison (CAI: chronic ankle instability group, CON: healthy control, Ant: anticipated landing-cutting, Unant: unanticipated landing-cutting)

			Synergy #1	Synergy #2	Synergy #3
CON Ant	vs.	CON Unant	0.85 ± 0.11	0.88 ± 0.10	0.88 ± 0.08
CON Ant	vs.	CAI Ant	0.84 ± 0.10	0.90 ± 0.09	0.89 ± 0.07
CON Unant	vs.	CAI Unant	0.86 ± 0.08	0.90 ± 0.06	0.90 ± 0.06
CAI Ant	vs.	CAI Unant	0.87 ± 0.07	0.91 ± 0.06	0.89 ± 0.06

The activation coefficient of Synergy 1 reflected muscle activation during the early and late stance phase of the cutting tasks. The muscle-specific weightings within the synergy vector of Synergy 1 reflected mainly TA activation. It therefore seems that Synergy 1 functions to control the ankle angle at ground contact and during late stance. The activation coefficient of Synergy 2 captured muscle activation during the middle stance phase of the cutting tasks, and the muscle-specific weightings within the synergy vector associated with this synergy indicated that it reflected primarily FL activation. Given that the FL acts primarily to evert the ankle in the frontal plane, the function of Synergy 2 thus seems to be related to the transition from forward to lateral motion during the mid-portion of the cutting tasks. Similarly, the activation coefficient of Synergy 3 also captured muscle activation in middle stance phase of the cutting tasks. Unlike synergy 2, however, the muscle-specific weightings within the synergy vector for Synergy 3 were associated with activation of the MG, LG, and SL. Thus, Synergy 3 seems to play propulsive role and helps accelerate the body towards the new cutting direction.

There were no significant group by task interactions for any of the individual muscle weightings for any of the synergy vectors and synergies. However, there were

significant main effects for group in the weightings for the TA and SL within the synergy vector of Synergy 1 (Figure 5. 3). Specifically, the task-averaged weightings of the TA were larger ($p = 0.023$) in the CAI group than in the CON group, whereas the task-averaged weightings of the SL were smaller ($p = 0.033$) in the CAI group than in the CON group. There were also significant main effects for task in the individual muscle weightings of the FL and MG within the synergy vector of Synergy 2 (Figure 5. 3). In particular, the group-averaged weightings of FL were smaller ($p = 0.029$) during Ant than Unant cutting, and the group-averaged weightings of MG were larger ($p = 0.032$) during Ant than during Unant cutting.

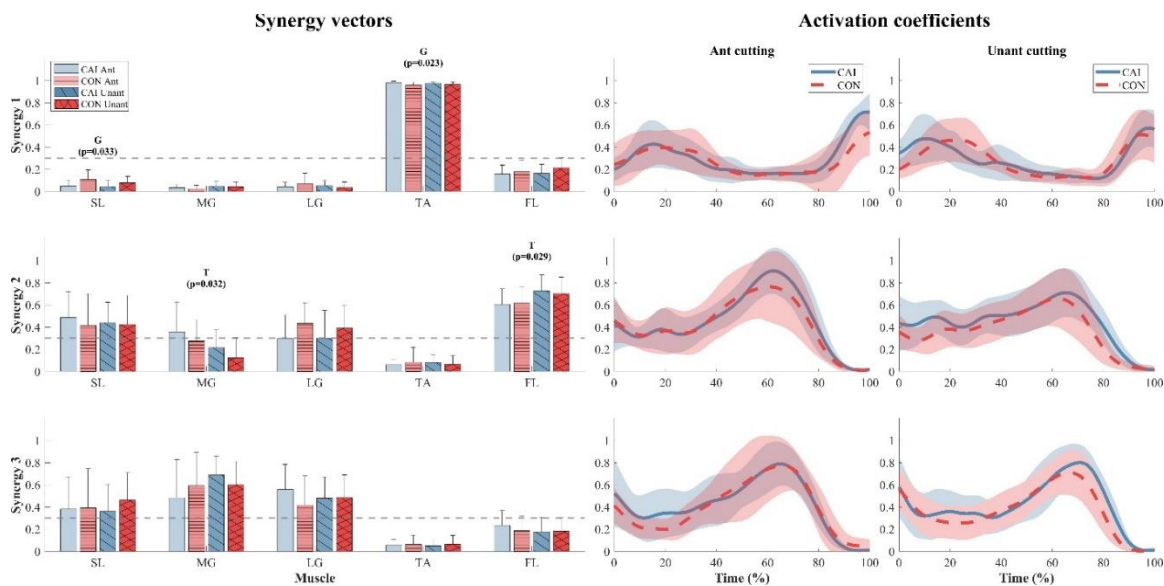


Figure 5. 3 Muscle synergy vectors (and muscle-specific weightings) and activation coefficients extracted from each group during each task (CAI: chronic ankle instability group, CON: healthy control, Ant: anticipated landing-cutting, Unant: unanticipated landing-cutting, SL: soleus, MG: medial gastrocnemius, LG: lateral gastrocnemius, TA: tibialis anterior, FL: fibularis longus, G: main effect for group, T: main effect for task).

DISCUSSION

The purposes of this study were to use NMF and extract muscle synergies in order to investigate and compare CNS-based neuromuscular control strategies in people with CAI and healthy CON during cutting tasks. The results showed that there was no significant difference in the dimensionality of muscle synergies between CAI and CON during Ant and Unant cutting tasks. While the first two muscle synergies were similar for both groups and tasks, a third synergy accounted for individual differences in both groups and tasks. People with CAI exhibited greater TA weightings and smaller SL weightings in Synergy 1 than people in CON group. Both groups exhibited smaller MG weightings and greater FL weightings in Synergy 2 during the Unant than Ant task. Together, these results partially supported our initial hypotheses in that people with CAI exhibited different weightings within specific muscle synergies, but this difference did not depend on task. Conversely, the results did not support our hypothesis that people with CAI used a different neuromuscular control strategy than CON.

The dimensionality of muscle synergies did not differ between the CAI and CON groups. This finding did not agree with our initial hypotheses that people with CAI would exhibit a smaller number of muscle synergies or that each muscle synergy would exhibit a greater VAF_{Total} . These hypotheses were based on research that suggested that people with neurological pathologies exhibit fewer muscle synergies and simpler neuromuscular control strategies (Safavynia et al., 2011). Fewer muscle synergies, as observed in people with neurological pathologies, may be due to greater co-contractions and result in less efficient movements (da Silva Costa, Moraes, Hortobagyi, & Sawers, 2020; Safavynia et al., 2011). However, since people in the CAI group exhibited the same number of muscle

synergies during both cutting tasks, it appears that they use a similar CNS-based neuromuscular control strategy during cutting tasks regardless of the associated cognitive load.

Analysis of the individual muscle weightings within each synergy indicated both group and task main effects. Specifically, within Synergy 1, the weighting of the TA muscle was greater for the CAI group than for the CON group, which indicates that people with CAI recruited the TA muscle to a greater extent than people in CON group. Given that the activation coefficient of Synergy 1 captured muscle activity during the early phase of stance during the cutting tasks, this result may suggest that people with CAI emphasize sagittal plane positioning of the ankle around touchdown or takeoff to a greater extent, which is clinically important as ankle positioning affects foot ground clearance and mitigates risk of unanticipated contact (C. Brown, 2011; Delahunt, Monaghan, & Caulfield, 2006a). In addition, computer simulations suggest that greater ankle dorsiflexion at the instance of foot contact is associated with a smaller external moment arm of the ground reaction forces about the subtalar joint, which could mitigate the risk of subsequent ankle sprains (I. C. Wright, Neptune, van den Bogert, & Nigg, 2000). In addition, a dorsiflexed position also increases stability of the ankle joint because the surfaces of the ankle joint become more congruent as dorsiflexion increases. People with CAI are thought to compensate for their lack of stability by dorsiflexing the ankle joint in order to achieve a more close-packed and stable position (Son et al., 2017). Lastly, greater emphasis on TA activation during the early stance phase may also increase coactivation and ankle joint stability (Baratta et al., 1988). Although group differences existed in the weighting of the SL for Synergy 1, the magnitudes of this weighting were very small (i.e., well below the

0.3 threshold) and may thus not reflect clinically or functionally important differences in muscle coordination between CAI and CON groups (Milosevic et al., 2017).

In addition to the group difference between CAI and CON in individual muscle weightings for Synergy 1, the results also revealed a task difference between the Ant and Unant task for Synergy 2. Specifically, both groups exhibited greater weighting of the FL and smaller weighting of the MG during Unant than during Ant cutting. Based on the timing of muscle activity, the activation coefficient for Synergy 2 suggests that people use this synergy to control muscle activation during the middle phase of stance during cutting. The increase in FL weighting may therefore reflect greater emphasis on transitioning from forward to lateral motion through greater activation of frontal plane muscles. In addition, greater FL weighting may also reflect an attempt to maintain balance and ankle joint stability in the frontal plane when the cutting task is performed with more uncertainty and without knowing the direction of movement (Meinerz, Malloy, Geiser, & Kipp, 2015). Interestingly, the increase in FL weighting was accompanied by a decrease in MG weighting – although, based on the thresholds, the changes in MG weighting within synergy 2 suggest that the MG would only be considered an ‘active’ muscle during the Ant task but not during the Unant task. Given that the MG is an important contributor to propulsive forces during cutting tasks (Maniar, Schache, Cole, & Opar, 2019), this change in neuromuscular control may further suggest that both groups emphasize frontal plane stability over cutting performance during the Unant task.

There are some limitations in the current study. First, we only recorded EMG from 5 lower leg muscles. A small number of muscles may lead to over-estimation of the VAF by NMF (Steele, Tresch, & Perreault, 2013). However, the 5 muscles in the current study

capture the major kinesiological functions of the ankle joint (i.e., plantar flexion, dorsiflexion, eversion), and thus likely still adequately represent neuromuscular strategies of ankle motions from a CNS control perspective. Considering that previous studies reported that people with CAI exhibit functional deficits in proximal muscles, it would be of value if future studies included these muscles (e.g., gluteus maximus) to better characterize, and more comprehensively understand, CNS control of muscle activation in people with CAI. Second, the current study included only people with CAI and healthy controls. Another group that is often studied in the literature are “copers” (e.g., those who have normal ankle functions after an initial ankle sprain). Investigating muscle synergies in “copers” may help further understand neuromuscular activation patterns and CNS control in people with CAI and may provide further insights for the development of rehabilitation strategies. Third, we analyzed only cutting tasks in a laboratory setting. Since ankle sprains can also occur during other movements (e.g., walking) or other environments (e.g., uneven/inclined surfaces), investigation of muscle synergies across a variety of tasks and conditions may also would reveal additional information that could hold important clinical implications.

CONCLUSION

Across the various Ant and Unant cutting tasks, people with CAI used global neuromuscular control strategies that were similar to healthy controls. However, regardless of cutting task people with CAI exhibited slight differences in how they recruited their ankle dorsiflexor muscles. Specifically, people with CAI relied on greater tibialis anterior weighting within the synergy that controlled muscle activation during the early and late

stance phase of cutting tasks. These findings suggest that although people with CAI exhibit similar complexity of CNS control during dynamic tasks, they also tune neuromuscular control strategy in muscle-specific manner that is consistent with mitigating risks of reinjury and increasing joint stability.

CHAPTER 6: CONCLUSION

The purpose of this dissertation was to study neuromuscular control in people with CAI using experimental and simulation approaches. Crucially, the series of four studies included in this dissertation clearly elucidated clinical implications related to muscle forces and force generating capacities (Chapter 2), contributions of muscles to ankle joint contact forces (Chapter 3), motor unit recruitment strategies (Chapter 4), and CNS control strategies (Chapter 5) during dynamic tasks in people with CAI compared to healthy controls. These studies also showed that musculoskeletal modeling and simulation, frequency analysis, and factorization techniques can be leveraged to answer clinically important knowledge gaps about neuromuscular deficits in people with CAI through the use of experimental data (e.g., motion capture data, EMG data). This chapter summarizes key findings of this dissertation and proposes directions for future studies.

The first study (Chapter 2) in this dissertation aimed to estimate the forces and force generating capacities of individual lower extremity muscles and to compare these estimates between people with and without CAI during landing and cutting tasks. We hypothesized that the peak muscle forces and force generating capacities would differ between groups and that these differences would be task-dependent. While previous studies revealed differences in terms of muscle strengths, these findings were based on single-joint dynamometry (e.g., Biodex) under isometric or isokinetic conditions. Although dynamometry represents a standard method to quantify the strength of isolated muscle groups (e.g., knee extensor strength) during a seated posture, it is difficult to measure the individual muscle forces during dynamic tasks. In addition, it is difficult to

understand how individual muscles generate force given force-length-velocity constraints behavior based on joint-specific kinematics during dynamic tasks. Thus, the simulation approach in the current study was used to estimate the individual muscle force and force generating capacity resulting from muscle behavior during landing-cutting tasks. The results showed that people with CAI exhibited greater force and force generating capacity of the gluteus maximus during all tasks and greater force generating capacity of the vastii muscles during unanticipated cutting compared to healthy controls. Interestingly, all significant differences were observed in proximal muscles (e.g., gluteus maximus and vastii) rather than distal muscles (e.g, soleus). This finding is consistent with previous studies where authors found proximal joint compensatory movement strategies in muscle activation, joint kinematics, and joint kinetics in people with CAI. This study enhanced the evidence of “proximal dominant landing strategy” in people with CAI by providing evidence regarding 1) individual muscle forces and 2) force generating capacity (i.e., muscle length-velocity-force behaviors). Therefore, these findings suggest that clinicians or coaches focus on restoring proximal movement patterns and muscular strengthening rather than just muscular strengthening in ankle joint muscles to prevent recurrent ankle injuries in people with CAI.

The second study (Chapter 3) in this dissertation investigated the contributions from muscle forces and GRF to ankle joint compression and anteroposterior shear forces in people with and without CAI during a cutting task. We hypothesized that the ankle joint compression and anteroposterior shear forces would be greater in people with CAI, and that the contribution of specific muscles to these forces would differ. Although epidemiological studies show that people with CAI tend to develop ankle osteoarthritis,

there is a research gap to identify the reason for the progression of ankle osteoarthritis in people with CAI. To seek possible solutions that prevent ankle osteoarthritis, investigating differences between people with and without CAI in specific risk factors of osteoarthritis appear warranted. Because ankle joint contact forces are a risk factor of progression of ankle osteoarthritis, ankle joint compression and anteroposterior shear forces were investigated in this study. In addition, because a recent study revealed that joint loads are strongly related to individual muscle forces, the contribution of individual muscle to joint contact force was also investigated in this study. The results showed that people with CAI exhibited greater anterior shear forces during the early and late phase of stance compared to CON. Specifically, the greater observed anterior shear forces during the early stance phase were the result of passive contributions from the GRF, while the greater anterior shear forces during late stance phase were the result of active contributions from lower leg muscles. These phase-specific differences were meaningful for understanding the mechanism behind greater joint loading in relation to joint contact forces in people with CAI compared to healthy controls. Although this study does not provide a direct link between CAI and OA, the results from the current study provide meaningful evidence for a framework that shows phase-specific increases of ankle anterior shear force and different contributions from GRF and lower leg muscles in people with CAI. This study suggests a future research direction to investigate if targeting the phase-specific contribution from GRF and lower leg muscles can decrease anterior shear force in relation to prevention of ankle osteoarthritis in people with CAI.

The third study (Chapter 4) in this dissertation identified differences in the time-frequency domain of muscle activation patterns between people with and without CAI

during athletic tasks (e.g., landing, anticipated cutting, and unanticipated cutting). We hypothesized that 1) there would be significant differences in the frequencies of muscle activation patterns between people with and without CAI and 2) that these differences would be task-dependent. Previous studies have thoroughly investigated deficits in peripheral nervous system and muscle activation patterns in people with CAI with tools such as EMG. Although previous studies revealed several findings about muscle activation and neuromuscular control, there was a research gap regarding motor unit recruitment strategies during dynamic tasks in people with CAI. Wavelet transform analysis was used in this study to identify the characteristics of muscle activation patterns in the time-frequency domain to provide clinical information about motor unit recruitment strategies. The results showed that people with CAI exhibited lower intensity across the entire frequency spectrum regardless of tasks and did not scale muscle activations towards higher frequencies during anticipated cutting. This research adds to growing evidence that people with CAI have not only lower intensity of muscle activations but also an inability to shift muscle activation towards higher frequency spectrum. The latter is clinically important because the inability to shift muscle activation towards higher frequency spectrum indicates that people with CAI may not be able to rapidly activate higher-threshold motor units in lower leg muscles during dynamic tasks. Based on this finding, it is suggested that clinicians and coaches should consider rehabilitation to facilitate fast contractions of lower leg muscles, given that activation of more fast motor units and greater firing rate are considered an important aspect in the prevention of injuries during dynamic tasks.

The fourth study (Chapter 5) in this dissertation investigated and compared CNS-based neuromuscular control strategies between people with CAI and healthy CON during cutting tasks. We hypothesized that people with CAI would 1) use fewer (i.e., less complex) muscle synergies, 2) exhibit different muscle-specific weightings within muscle synergies, and 3) display task-specific differences in these muscle synergies. In contrast to a lot of previous work on CAI related deficits in peripheral nervous system function, there is a lack of information about CNS deficits in people with CAI. The main reason for the lack of evidence about CNS deficits in people with CAI is a limited access to measure CNS signals during dynamic tasks. In this study, NMF (i.e., a matrix factorization technique) was used to extract muscle synergies based on experimentally measured muscle activations during anticipated and unanticipated cutting tasks. The results showed that people with CAI control their movements with similar complexity but different weightings for specific muscles. Specifically, people with CAI exhibited CNS control strategies in relation to diminishing risks of recurrent ankle injuries by recruiting the tibialis anterior muscle with greater weightings via a descending signal, which likely helps to make the ankle joint more stable during the early stance phase. This study enhanced the body of literature about neuromuscular control in people with CAI by confirming that CNS control of neuromuscular activation patterns in people with CAI controls exhibits a similar complexity but manifests in a more protective manner in the ankle joint compared to healthy controls.

Despite novel findings from each of the four studies in this dissertation, there are limitations to be considered. First, activations were measured from only five lower leg muscles. Although we found meaningful differences in neuromuscular characteristics in

people with CAI, including EMG from proximal muscles such as gluteus maximus, hamstrings, or quadriceps would provide a broader spectrum of information about neuromuscular movement strategies. In particular, including proximal muscles as well as distal muscles would provide information about motor unit recruitment strategies and muscle synergies in time-frequency and NMF analysis, respectively. In addition, including more muscles would provide an additional data for validating simulated muscle activations (Chapter 2 and Chapter 3). Second, a more realistic musculoskeletal model is necessary for future studies. In the first two studies (Chapter 2 and Chapter 3), the muscle forces and joint contact forces were estimated based on generic muscle parameters, except for maximum isometric muscle forces. A recent study revealed that the muscle forces and joint contact forces are strongly related to muscle parameters such as optimal muscle fiber lengths, tendon slack lengths, and muscle moment arms (Serrancolí, Kinney, & Fregly, 2020). Thus, modeling muscles with subject-specific parameters would provide more accurate findings about muscle forces and joint contact forces. In addition, the musculoskeletal model we used in the first two studies included an ankle-foot complex with 2 segments: a talus segment and a foot segment (calcaneus to toe). Since a recent study revealed that a model with at least 3 segments (talus, calcaneus to metatarsal bone, and separate toe) may be more adequate for calculating ankle joint kinematics, muscle lengths, and ligament lengths during dynamic performances (Kim & Kipp, 2020), a multisegment foot model should therefore be considered in future studies. Third, this dissertation did not recruit copers who have a history of ankle sprain but have no CAI or neuromuscular deficits. Recruiting a group of copers as well as people with CAI and healthy controls would provide more detailed neuromuscular characteristics of CAI

because previous studies revealed that people with CAI have different sensorimotor function compared to copers (Wikstrom et al., 2012).

In summary, this dissertation demonstrated that people with CAI have different neuromuscular control strategies during landing and cutting tasks compared to healthy controls. Specifically, people with CAI exhibit 1) greater muscle forces and force generating capacities of the gluteus maximus and greater task-dependent force generating capacities of the vastii muscles, 2) greater ankle anterior shear forces during early and late phase during unanticipated cutting due to respectively greater phase-specific GRF and lower leg muscle forces, 3) lower overall intensity of ankle muscle activation and a task-dependent inability to shift activation towards higher frequencies, and 4) similar complexity in CNS-based neuromuscular control strategy but with greater tibialis anterior specific weightings and activations during the early stance phase of cutting tasks.

BIBLIOGRAPHY

- Alentorn-Geli, E., Myer, G. D., Silvers, H. J., Samitier, G., Romero, D., Lazaro-Haro, C., & Cugat, R. (2009). Prevention of non-contact anterior cruciate ligament injuries in soccer players. Part 1: Mechanisms of injury and underlying risk factors. *Knee Surg Sports Traumatol Arthrosc*, *17*(7), 705-729. doi:10.1007/s00167-009-0813-1
- Allen, J. L., Kesar, T. M., & Ting, L. H. (2019). Motor module generalization across balance and walking is impaired after stroke. *J Neurophysiol*, *122*(1), 277-289. doi:10.1152/jn.00561.2018
- Arnold, E. M., Hamner, S. R., Seth, A., Millard, M., & Delp, S. L. (2013). How muscle fiber lengths and velocities affect muscle force generation as humans walk and run at different speeds. *J Exp Biol*, *216*(Pt 11), 2150-2160. doi:10.1242/jeb.075697
- Attenborough, A. S., Hiller, C. E., Smith, R. M., Stuelcken, M., Greene, A., & Sinclair, P. J. (2014). Chronic ankle instability in sporting populations. *Sports Med*, *44*(11), 1545-1556. doi:10.1007/s40279-014-0218-2
- Bae, J. Y., Park, K. S., Seon, J. K., & Jeon, I. (2015). Analysis of the Effects of Normal Walking on Ankle Joint Contact Characteristics After Acute Inversion Ankle Sprain. *Ann Biomed Eng*, *43*(12), 3015-3024. doi:10.1007/s10439-015-1360-1
- Banks, C. L., Pai, M. M., McGuirk, T. E., Fregly, B. J., & Patten, C. (2017). Methodological Choices in Muscle Synergy Analysis Impact Differentiation of Physiological Characteristics Following Stroke. *Front Comput Neurosci*, *11*, 78. doi:10.3389/fncom.2017.00078
- Baratta, R., Solomonow, M., Zhou, B. H., Letson, D., Chuinard, R., & D'Ambrosia, R. (1988). Muscular coactivation. The role of the antagonist musculature in maintaining knee stability. *Am J Sports Med*, *16*(2), 113-122. doi:10.1177/036354658801600205
- Boccia, G., Zoppirolli, C., Bortolan, L., Schena, F., & Pellegrini, B. (2018). Shared and task-specific muscle synergies of Nordic walking and conventional walking. *Scand J Med Sci Sports*, *28*(3), 905-918. doi:10.1111/sms.12992
- Briggs, K. K., Lysholm, J., Tegner, Y., Rodkey, W. G., Kocher, M. S., & Steadman, J. R. (2009). The reliability, validity, and responsiveness of the Lysholm score and

Tegner activity scale for anterior cruciate ligament injuries of the knee: 25 years later. *Am J Sports Med*, 37(5), 890-897. doi:10.1177/0363546508330143

Brown, C. (2011). Foot clearance in walking and running in individuals with ankle instability. *Am J Sports Med*, 39(8), 1769-1776. doi:10.1177/0363546511408872

Brown, C., Padua, D., Marshall, S. W., & Guskiewicz, K. (2008). Individuals with mechanical ankle instability exhibit different motion patterns than those with functional ankle instability and ankle sprain copers. *Clin Biomech (Bristol, Avon)*, 23(6), 822-831. doi:10.1016/j.clinbiomech.2008.02.013

Brown, T. N., Palmieri-Smith, R. M., & McLean, S. G. (2009). Sex and limb differences in hip and knee kinematics and kinetics during anticipated and unanticipated jump landings: implications for anterior cruciate ligament injury. *Br J Sports Med*, 43(13), 1049-1056. doi:10.1136/bjsm.2008.055954

Buchthal, F., Guld, C., & Rosenfalck, P. (1955). Innervation zone and propagation velocity in human muscle. *Acta Physiol Scand*, 35(2), 174-190. doi:10.1111/j.1748-1716.1955.tb01276.x

Caputo, A. M., Lee, J. Y., Spritzer, C. E., Easley, M. E., DeOrto, J. K., Nunley, J. A., 2nd, & DeFrate, L. E. (2009). In vivo kinematics of the tibiotalar joint after lateral ankle instability. *Am J Sports Med*, 37(11), 2241-2248. doi:10.1177/0363546509337578

Carbone, A., & Rodeo, S. (2017). Review of current understanding of post-traumatic osteoarthritis resulting from sports injuries. *J Orthop Res*, 35(3), 397-405. doi:10.1002/jor.23341

Caulfield, B. M., & Garrett, M. (2002). Functional instability of the ankle: differences in patterns of ankle and knee movement prior to and post landing in a single leg jump. *Int J Sports Med*, 23(1), 64-68. doi:10.1055/s-2002-19272

Chvatal, S. A., & Ting, L. H. (2013). Common muscle synergies for balance and walking. *Front Comput Neurosci*, 7, 48. doi:10.3389/fncom.2013.00048

Clark, D. J., Ting, L. H., Zajac, F. E., Neptune, R. R., & Kautz, S. A. (2010). Merging of healthy motor modules predicts reduced locomotor performance and muscle coordination complexity post-stroke. *J Neurophysiol*, 103(2), 844-857. doi:10.1152/jn.00825.2009

- Cleather, D. J., Goodwin, J. E., & Bull, A. M. (2013). Hip and knee joint loading during vertical jumping and push jerking. *Clin Biomech (Bristol, Avon)*, 28(1), 98-103. doi:10.1016/j.clinbiomech.2012.10.006
- Cohen, J. (2013). *Statistical power analysis for the behavioral sciences*: Academic press.
- Cohen, N. P., Foster, R. J., & Mow, V. C. (1998). Composition and dynamics of articular cartilage: structure, function, and maintaining healthy state. *J Orthop Sports Phys Ther*, 28(4), 203-215. doi:10.2519/jospt.1998.28.4.203
- Conforto, S., D'Alessio, T., & Pignatelli, S. (1999). Optimal rejection of movement artefacts from myoelectric signals by means of a wavelet filtering procedure. *J Electromyogr Kinesiol*, 9(1), 47-57.
- Corcos, D. M., Gottlieb, G. L., Latash, M. L., Almeida, G. L., & Agarwal, G. C. (1992). Electromechanical delay: An experimental artifact. *J Electromyogr Kinesiol*, 2(2), 59-68. doi:10.1016/1050-6411(92)90017-D
- d'Avella, A., Saltiel, P., & Bizzi, E. (2003). Combinations of muscle synergies in the construction of a natural motor behavior. *Nat Neurosci*, 6(3), 300-308. doi:10.1038/nn1010
- da Silva Costa, A. A., Moraes, R., Hortobagyi, T., & Sawers, A. (2020). Older adults reduce the complexity and efficiency of neuromuscular control to preserve walking balance. *Exp Gerontol*, 140, 111050. doi:10.1016/j.exger.2020.111050
- DeJong, A. F., Mangum, L. C., & Hertel, J. (2019). Gluteus medius activity during gait is altered in individuals with chronic ankle instability: An ultrasound imaging study. *Gait Posture*, 71, 7-13. doi:10.1016/j.gaitpost.2019.04.007
- DeJong, A. F., Mangum, L. C., & Hertel, J. (2020). Ultrasound Imaging of the Gluteal Muscles During the Y-Balance Test in Individuals With or Without Chronic Ankle Instability. *J Athl Train*, 55(1), 49-57. doi:10.4085/1062-6050-363-18
- Delahunt, E., Monaghan, K., & Caulfield, B. (2006a). Altered neuromuscular control and ankle joint kinematics during walking in subjects with functional instability of the ankle joint. *Am J Sports Med*, 34(12), 1970-1976. doi:10.1177/0363546506290989

- Delahunt, E., Monaghan, K., & Caulfield, B. (2006b). Changes in lower limb kinematics, kinetics, and muscle activity in subjects with functional instability of the ankle joint during a single leg drop jump. *J Orthop Res*, *24*(10), 1991-2000. doi:10.1002/jor.20235
- Delp, S. L., Anderson, F. C., Arnold, A. S., Loan, P., Habib, A., John, C. T., . . . Thelen, D. G. (2007). OpenSim: open-source software to create and analyze dynamic simulations of movement. *IEEE Trans Biomed Eng*, *54*(11), 1940-1950. doi:10.1109/TBME.2007.901024
- Delp, S. L., Loan, J. P., Hoy, M. G., Zajac, F. E., Topp, E. L., & Rosen, J. M. (1990). An interactive graphics-based model of the lower extremity to study orthopaedic surgical procedures. *IEEE Trans Biomed Eng*, *37*(8), 757-767. doi:10.1109/10.102791
- Docherty, C. L., Gansneder, B. M., Arnold, B. L., & Hurwitz, S. R. (2006). Development and reliability of the ankle instability instrument. *J Athl Train*, *41*(2), 154-158.
- Doherty, C., Bleakley, C., Hertel, J., Caulfield, B., Ryan, J., & Delahunt, E. (2016). Single-leg drop landing movement strategies in participants with chronic ankle instability compared with lateral ankle sprain 'copers'. *Knee Surg Sports Traumatol Arthrosc*, *24*(4), 1049-1059. doi:10.1007/s00167-015-3852-9
- Donnelly, L., Donovan, L., Hart, J. M., & Hertel, J. (2017). Eversion Strength and Surface Electromyography Measures With and Without Chronic Ankle Instability Measured in 2 Positions. *Foot Ankle Int*, *38*(7), 769-778. doi:10.1177/1071100717701231
- Feger, M. A., Donovan, L., Hart, J. M., & Hertel, J. (2015). Lower extremity muscle activation in patients with or without chronic ankle instability during walking. *J Athl Train*, *50*(4), 350-357. doi:10.4085/1062-6050-50.2.06
- Field, A. (2013). *Discovering statistics using IBM SPSS statistics*: sage.
- Flevas, D. A., Bernard, M., Ristanis, S., Moraiti, C., Georgoulis, A. D., & Pappas, E. (2017). Peroneal electromechanical delay and fatigue in patients with chronic ankle instability. *Knee Surg Sports Traumatol Arthrosc*, *25*(6), 1903-1907. doi:10.1007/s00167-016-4243-6

- Gribble, P. A., Bleakley, C. M., Caulfield, B. M., Docherty, C. L., Fourchet, F., Fong, D. T., . . . Delahunt, E. (2016). Evidence review for the 2016 International Ankle Consortium consensus statement on the prevalence, impact and long-term consequences of lateral ankle sprains. *Br J Sports Med*, *50*(24), 1496-1505. doi:10.1136/bjsports-2016-096189
- Gribble, P. A., Delahunt, E., Bleakley, C. M., Caulfield, B., Docherty, C. L., Fong, D. T., . . . Wikstrom, E. A. (2014). Selection criteria for patients with chronic ankle instability in controlled research: a position statement of the International Ankle Consortium. *J Athl Train*, *49*(1), 121-127. doi:10.4085/1062-6050-49.1.14
- Gribble, P. A., & Robinson, R. H. (2009). Alterations in knee kinematics and dynamic stability associated with chronic ankle instability. *J Athl Train*, *44*(4), 350-355. doi:10.4085/1062-6050-44.4.350
- Hale, S. A., & Hertel, J. (2005). Reliability and Sensitivity of the Foot and Ankle Disability Index in Subjects With Chronic Ankle Instability. *J Athl Train*, *40*(1), 35-40.
- Hamner, S. R., & Delp, S. L. (2013). Muscle contributions to fore-aft and vertical body mass center accelerations over a range of running speeds. *J Biomech*, *46*(4), 780-787. doi:10.1016/j.jbiomech.2012.11.024
- Hamner, S. R., Seth, A., & Delp, S. L. (2010). Muscle contributions to propulsion and support during running. *J Biomech*, *43*(14), 2709-2716. doi:10.1016/j.jbiomech.2010.06.025
- Handsfield, G. G., Meyer, C. H., Hart, J. M., Abel, M. F., & Blemker, S. S. (2014). Relationships of 35 lower limb muscles to height and body mass quantified using MRI. *J Biomech*, *47*(3), 631-638. doi:10.1016/j.jbiomech.2013.12.002
- Herb, C. C., Grossman, K., Feger, M. A., Donovan, L., & Hertel, J. (2018). Lower Extremity Biomechanics During a Drop-Vertical Jump in Participants With or Without Chronic Ankle Instability. *J Athl Train*, *53*(4), 364-371. doi:10.4085/1062-6050-481-15
- Hertel, J. (2002). Functional Anatomy, Pathomechanics, and Pathophysiology of Lateral Ankle Instability. *J Athl Train*, *37*(4), 364-375.

- Hertel, J., & Corbett, R. O. (2019). An Updated Model of Chronic Ankle Instability. *J Athl Train*, 54(6), 572-588. doi:10.4085/1062-6050-344-18
- Herzog, M. M., Kerr, Z. Y., Marshall, S. W., & Wikstrom, E. A. (2019). Epidemiology of Ankle Sprains and Chronic Ankle Instability. *J Athl Train*, 54(6), 603-610. doi:10.4085/1062-6050-447-17
- Herzog, W., Longino, D., & Clark, A. (2003). The role of muscles in joint adaptation and degeneration. *Langenbecks Arch Surg*, 388(5), 305-315. doi:10.1007/s00423-003-0402-6
- Hicks, J. L., Uchida, T. K., Seth, A., Rajagopal, A., & Delp, S. L. (2015). Is my model good enough? Best practices for verification and validation of musculoskeletal models and simulations of movement. *J Biomech Eng*, 137(2), 020905. doi:10.1115/1.4029304
- Hintermann, B., Boss, A., & Schafer, D. (2002). Arthroscopic findings in patients with chronic ankle instability. *Am J Sports Med*, 30(3), 402-409. doi:10.1177/03635465020300031601
- Hoch, M. C., & McKeon, P. O. (2014). Peroneal reaction time after ankle sprain: a systematic review and meta-analysis. *Med Sci Sports Exerc*, 46(3), 546-556. doi:10.1249/MSS.0b013e3182a6a93b
- Hopkins, J. T., Brown, T. N., Christensen, L., & Palmieri-Smith, R. M. (2009). Deficits in peroneal latency and electromechanical delay in patients with functional ankle instability. *J Orthop Res*, 27(12), 1541-1546. doi:10.1002/jor.20934
- Houston, M. N., Hoch, J. M., & Hoch, M. C. (2015). Patient-Reported Outcome Measures in Individuals With Chronic Ankle Instability: A Systematic Review. *J Athl Train*, 50(10), 1019-1033. doi:10.4085/1062-6050-50.9.01
- Houston, M. N., Van Lunen, B. L., & Hoch, M. C. (2014). Health-related quality of life in individuals with chronic ankle instability. *J Athl Train*, 49(6), 758-763. doi:10.4085/1062-6050-49.3.54
- Hubbard-Turner, T. (2012). Relationship between mechanical ankle joint laxity and subjective function. *Foot Ankle Int*, 33(10), 852-856. doi:DOI: 10.3113/FAI.2012.0852
10.3113/FAI.2012.0852

- Hubbard, T. J., & Wikstrom, E. A. (2010). Ankle sprain: pathophysiology, predisposing factors, and management strategies. *Open Access J Sports Med, 1*, 115-122.
- Humphrey, D. R., & Reed, D. J. (1983). Separate cortical systems for control of joint movement and joint stiffness: reciprocal activation and coactivation of antagonist muscles. *Adv Neurol, 39*, 347-372.
- Hunter, D. J., & Eckstein, F. (2009). Exercise and osteoarthritis. *J Anat, 214*(2), 197-207. doi:10.1111/j.1469-7580.2008.01013.x
- Jewell, C., Hamill, J., von Tscharnner, V., & Boyer, K. A. (2019). Altered multi-muscle coordination patterns in habitual forefoot runners during a prolonged, exhaustive run. *Eur J Sport Sci, 19*(8), 1062-1071. doi:10.1080/17461391.2019.1575912
- Karabulut, D., Dogru, S. C., Lin, Y. C., Pandy, M., Herzog, W., & Arslan, Y. Z. (2019). Direct Validation of Model-predicted Muscle Forces in the Cat Hindlimb During Walking. *J Biomech Eng.* doi:10.1115/1.4045660
- Kim, H., & Kipp, K. (2019). Number of Segments Within Musculoskeletal Foot Models Influences Ankle Kinematics and Strains of Ligaments and Muscles. *J Orthop Res, 37*(10), 2231-2240. doi:10.1002/jor.24394
- Kim, H., & Kipp, K. (2020). Simulated anterior translation and medial rotation of the talus affect ankle joint contact forces during vertical hopping. *Comput Methods Biomech Biomed Engin, 23*(9), 484-490. doi:10.1080/10255842.2020.1738405
- Kim, H., Palmieri-Smith, R., & Kipp, K. (2020). Time-frequency analysis of muscle activation patterns in people with chronic ankle instability during Landing and cutting tasks. *Gait Posture, 82*, 203-208. doi:10.1016/j.gaitpost.2020.09.006
- Kim, H., Son, S. J., Seeley, M. K., & Hopkins, J. T. (2019). Altered movement strategies during jump landing/cutting in patients with chronic ankle instability. *Scand J Med Sci Sports, 29*(8), 1130-1140. doi:10.1111/sms.13445
- Kim, K.-M., Ingersoll, C. D., & Hertel, J. (2012). Altered postural modulation of Hoffmann reflex in the soleus and fibularis longus associated with chronic ankle instability. *Journal of Electromyography and Kinesiology, 22*(6), 997-1002.

- Kipp, K., & Palmieri-Smith, R. M. (2012). Principal component based analysis of biomechanical inter-trial variability in individuals with chronic ankle instability. *Clin Biomech (Bristol, Avon)*, 27(7), 706-710. doi:10.1016/j.clinbiomech.2012.02.005
- Kipp, K., & Palmieri-Smith, R. M. (2013). Differences in kinematic control of ankle joint motions in people with chronic ankle instability. *Clin Biomech (Bristol, Avon)*, 28(5), 562-567. doi:10.1016/j.clinbiomech.2013.03.008
- Kuntze, G., von Tscharnner, V., Hutchison, C., & Ronsky, J. L. (2015). Multi-muscle activation strategies during walking in female post-operative total joint replacement patients. *J Electromyogr Kinesiol*, 25(4), 715-721. doi:10.1016/j.jelekin.2015.04.001
- Kunugi, S., Masunari, A., Koumura, T., Fujimoto, A., Yoshida, N., & Miyakawa, S. (2018). Altered lower limb kinematics and muscle activities in soccer players with chronic ankle instability. *Phys Ther Sport*, 34, 28-35. doi:10.1016/j.pts.2018.08.003
- Kwon, Y. U., Harrison, K., Kweon, S. J., & Blaise Williams, D. S., 3rd. (2019). Ankle Coordination in Chronic Ankle Instability, Coper, and Control Groups in Running. *Med Sci Sports Exerc.* doi:10.1249/MSS.0000000000002170
- Lai, A., Schache, A. G., Brown, N. A., & Pandy, M. G. (2016). Human ankle plantar flexor muscle-tendon mechanics and energetics during maximum acceleration sprinting. *J R Soc Interface*, 13(121). doi:10.1098/rsif.2016.0391
- Lane Smith, R., Trindade, M. C., Ikenoue, T., Mohtai, M., Das, P., Carter, D. R., . . . Schurman, D. J. (2000). Effects of shear stress on articular chondrocyte metabolism. *Biorheology*, 37(1-2), 95-107.
- Lee, D. D., & Seung, H. S. (1999). Learning the parts of objects by non-negative matrix factorization. *Nature*, 401(6755), 788-791. doi:10.1038/44565
- Lee, S. S., de Boef Miara, M., Arnold, A. S., Biewener, A. A., & Wakeling, J. M. (2013). Recruitment of faster motor units is associated with greater rates of fascicle strain and rapid changes in muscle force during locomotion. *J Exp Biol*, 216(Pt 2), 198-207. doi:10.1242/jeb.072637

- Lenton, G. K., Bishop, P. J., Saxby, D. J., Doyle, T. L. A., Pizzolato, C., Billing, D., & Lloyd, D. G. (2018). Tibiofemoral joint contact forces increase with load magnitude and walking speed but remain almost unchanged with different types of carried load. *PLoS One*, *13*(11), e0206859. doi:10.1371/journal.pone.0206859
- Li, Y., Wang, H., & Simpson, K. J. (2019). Chronic Ankle Instability Does Not Influence Tibiofemoral Contact Forces During Drop Landings Using a Musculoskeletal Model. *J Appl Biomech*, 1-5. doi:10.1123/jab.2018-0436
- Mangum, L. C., Henderson, K., Murray, K. P., & Saliba, S. A. (2018). Ultrasound Assessment of the Transverse Abdominis During Functional Movement. *J Ultrasound Med*, *37*(5), 1225-1231. doi:10.1002/jum.14466
- Maniar, N., Schache, A. G., Cole, M. H., & Opar, D. A. (2019). Lower-limb muscle function during sidestep cutting. *J Biomech*, *82*, 186-192. doi:10.1016/j.jbiomech.2018.10.021
- Maniar, N., Schache, A. G., Sritharan, P., & Opar, D. A. (2018). Non-knee-spanning muscles contribute to tibiofemoral shear as well as valgus and rotational joint reaction moments during unanticipated sidestep cutting. *Sci Rep*, *8*(1), 2501. doi:10.1038/s41598-017-19098-9
- McCann, R. S., Terada, M., Kosik, K. B., & Gribble, P. A. (2019). Landing Kinematics and Isometric Hip Strength of Individuals With Chronic Ankle Instability. *Foot Ankle Int*, *40*(8), 969-977. doi:10.1177/1071100719846085
- McKay, G. D., Goldie, P. A., Payne, W. R., & Oakes, B. W. (2001). Ankle injuries in basketball: injury rate and risk factors. *Br J Sports Med*, *35*(2), 103-108. doi:10.1136/bjism.35.2.103
- McLeod, M. M., Gribble, P. A., & Pietrosimone, B. G. (2015). Chronic Ankle Instability and Neural Excitability of the Lower Extremity. *J Athl Train*, *50*(8), 847-853. doi:10.4085/1062-6050-50.4.06
- McVey, E. D., Palmieri, R. M., Docherty, C. L., Zinder, S. M., & Ingersoll, C. D. (2005). Arthrogenic muscle inhibition in the leg muscles of subjects exhibiting functional ankle instability. *Foot Ankle Int*, *26*(12), 1055-1061. doi:10.1177/107110070502601210

- Meinerz, C. M., Malloy, P., Geiser, C. F., & Kipp, K. (2015). Anticipatory Effects on Lower Extremity Neuromechanics During a Cutting Task. *J Athl Train, 50*(9), 905-913. doi:10.4085/1062-6050-50.8.02
- Milosevic, M., Yokoyama, H., Grangeon, M., Masani, K., Popovic, M. R., Nakazawa, K., & Gagnon, D. H. (2017). Muscle synergies reveal impaired trunk muscle coordination strategies in individuals with thoracic spinal cord injury. *J Electromyogr Kinesiol, 36*, 40-48. doi:10.1016/j.jelekin.2017.06.007
- Minoonejad, H., Karimizadeh Ardakani, M., Rajabi, R., Wikstrom, E. A., & Sharifnezhad, A. (2019). Hop Stabilization Training Improves Neuromuscular Control in College Basketball Players With Chronic Ankle Instability: A Randomized Controlled Trial. *J Sport Rehabil, 28*(6), 576-583. doi:10.1123/jsr.2018-0103
- Mohr, M., von Tscherner, V., Emery, C. A., & Nigg, B. M. (2019). Classification of gait muscle activation patterns according to knee injury history using a support vector machine approach. *Hum Mov Sci, 66*, 335-346. doi:10.1016/j.humov.2019.05.006
- Monaghan, K., Delahunt, E., & Caulfield, B. (2006). Ankle function during gait in patients with chronic ankle instability compared to controls. *Clin Biomech (Bristol, Avon), 21*(2), 168-174. doi:10.1016/j.clinbiomech.2005.09.004
- Munn, J., Sullivan, S. J., & Schneiders, A. G. (2010). Evidence of sensorimotor deficits in functional ankle instability: a systematic review with meta-analysis. *J Sci Med Sport, 13*(1), 2-12. doi:10.1016/j.jsams.2009.03.004
- Needle, A. R., Lepley, A. S., & Grooms, D. R. (2017). Central Nervous System Adaptation After Ligamentous Injury: a Summary of Theories, Evidence, and Clinical Interpretation. *Sports Med, 47*(7), 1271-1288. doi:10.1007/s40279-016-0666-y
- Needle, A. R., Palmer, J. A., Kesar, T. M., Binder-Macleod, S. A., & Swanik, C. B. (2013). Brain regulation of muscle tone in healthy and functionally unstable ankles. *J Sport Rehabil, 22*(3), 202-211. doi:10.1123/jsr.22.3.202
- O'Driscoll, J., & Delahunt, E. (2011). Neuromuscular training to enhance sensorimotor and functional deficits in subjects with chronic ankle instability: A systematic review and best evidence synthesis. *Sports Med Arthrosc Rehabil Ther Technol, 3*, 19. doi:10.1186/1758-2555-3-19

- Öner, M., & Deveci Kocakoç, İ. (2017). Jmasm 49: A compilation of some popular goodness of fit tests for normal distribution: Their algorithms and matlab codes (matlab). *Journal of Modern Applied Statistical Methods*, 16(2), 30.
- Rabbi, M. F., Pizzolato, C., Lloyd, D. G., Carty, C. P., Devaprakash, D., & Diamond, L. E. (2020). Non-negative matrix factorisation is the most appropriate method for extraction of muscle synergies in walking and running. *Sci Rep*, 10(1), 8266. doi:10.1038/s41598-020-65257-w
- Radwan, A., Bakowski, J., Dew, S., Greenwald, B., Hyde, E., & Webber, N. (2016). Effectiveness of Ultrasonography in Diagnosing Chronic Lateral Ankle Instability:A Systematic Review. *Int J Sports Phys Ther*, 11(2), 164-174.
- Rios, J. L., Gorges, A. L., & dos Santos, M. J. (2015). Individuals with chronic ankle instability compensate for their ankle deficits using proximal musculature to maintain reduced postural sway while kicking a ball. *Hum Mov Sci*, 43, 33-44. doi:10.1016/j.humov.2015.07.001
- Rosen, A., Swanik, C., Thomas, S., Glutting, J., Knight, C., & Kaminski, T. W. (2013). Differences in lateral drop jumps from an unknown height among individuals with functional ankle instability. *J Athl Train*, 48(6), 773-781. doi:10.4085/1062-6050-48.5.05
- Rosen, A. B., Yentes, J. M., McGrath, M. L., Maerlender, A. C., Myers, S. A., & Mukherjee, M. (2019). Alterations in Cortical Activation Among Individuals With Chronic Ankle Instability During Single-Limb Postural Control. *J Athl Train*, 54(6), 718-726. doi:10.4085/1062-6050-448-17
- Safavynia, S. A., Torres-Oviedo, G., & Ting, L. H. (2011). Muscle Synergies: Implications for Clinical Evaluation and Rehabilitation of Movement. *Top Spinal Cord Inj Rehabil*, 17(1), 16-24. doi:10.1310/sci1701-16
- Sasaki, K., & Neptune, R. R. (2010). Individual muscle contributions to the axial knee joint contact force during normal walking. *J Biomech*, 43(14), 2780-2784. doi:10.1016/j.jbiomech.2010.06.011
- Serrancolí, G., Kinney, A. L., & Fregly, B. J. (2020). Influence of Musculoskeletal Model Parameter Values on Prediction of Accurate Knee Contact Forces during Walking. *Medical Engineering & Physics*.

- Shuman, B. R., Goudriaan, M., Desloovere, K., Schwartz, M. H., & Steele, K. M. (2019). Muscle synergies demonstrate only minimal changes after treatment in cerebral palsy. *J Neuroeng Rehabil*, 16(1), 46. doi:10.1186/s12984-019-0502-3
- Simpson, J. D., Koldenhoven, R. M., Wilson, S. J., Stewart, E. M., Turner, A. J., Chander, H., & Knight, A. C. (2020). Ankle kinematics, center of pressure progression, and lower extremity muscle activity during a side-cutting task in participants with and without chronic ankle instability. *Journal of Electromyography and Kinesiology*, 102454.
- Simpson, J. D., Stewart, E. M., Macias, D. M., Chander, H., & Knight, A. C. (2019). Individuals with chronic ankle instability exhibit dynamic postural stability deficits and altered unilateral landing biomechanics: A systematic review. *Phys Ther Sport*, 37, 210-219. doi:10.1016/j.ptsp.2018.06.003
- Son, S. J., Kim, H., Seeley, M. K., & Hopkins, J. T. (2017). Movement Strategies among Groups of Chronic Ankle Instability, Coper, and Control. *Med Sci Sports Exerc*, 49(8), 1649-1661. doi:10.1249/MSS.0000000000001255
- Son, S. J., Kim, H., Seeley, M. K., & Hopkins, J. T. (2019). Altered Walking Neuromechanics in Patients With Chronic Ankle Instability. *J Athl Train*, 54(6), 684-697. doi:10.4085/1062-6050-478-17
- Song, K., Rhodes, E., & Wikstrom, E. A. (2018). Balance Training Does Not Alter Reliance on Visual Information during Static Stance in Those with Chronic Ankle Instability: A Systematic Review with Meta-Analysis. *Sports Med*, 48(4), 893-905. doi:10.1007/s40279-017-0850-8
- Steele, K. M., Demers, M. S., Schwartz, M. H., & Delp, S. L. (2012). Compressive tibiofemoral force during crouch gait. *Gait Posture*, 35(4), 556-560. doi:10.1016/j.gaitpost.2011.11.023
- Steele, K. M., Tresch, M. C., & Perreault, E. J. (2013). The number and choice of muscles impact the results of muscle synergy analyses. *Front Comput Neurosci*, 7, 105. doi:10.3389/fncom.2013.00105
- Suttmiller, A. M. B., & McCann, R. S. (2020). Neural excitability of lower extremity musculature in individuals with and without chronic ankle instability: A systematic review and meta-analysis. *J Electromyogr Kinesiol*, 53, 102436. doi:10.1016/j.jelekin.2020.102436

- Swanik, C. B., Covassin, T., Stearne, D. J., & Schatz, P. (2007). The relationship between neurocognitive function and noncontact anterior cruciate ligament injuries. *Am J Sports Med*, 35(6), 943-948. doi:10.1177/0363546507299532
- Tabrizi, P., McIntyre, W. M., Quesnel, M. B., & Howard, A. W. (2000). Limited dorsiflexion predisposes to injuries of the ankle in children. *J Bone Joint Surg Br*, 82(8), 1103-1106. doi:10.1302/0301-620x.82b8.10134
- Tanen, L., Docherty, C. L., Van Der Pol, B., Simon, J., & Schrader, J. (2014). Prevalence of chronic ankle instability in high school and division I athletes. *Foot Ankle Spec*, 7(1), 37-44. doi:10.1177/1938640013509670
- Terada, M., Pietrosimone, B., & Gribble, P. A. (2014). Individuals with chronic ankle instability exhibit altered landing knee kinematics: potential link with the mechanism of loading for the anterior cruciate ligament. *Clin Biomech (Bristol, Avon)*, 29(10), 1125-1130. doi:10.1016/j.clinbiomech.2014.09.014
- Theisen, A., & Day, J. (2019). Chronic Ankle Instability Leads to Lower Extremity Kinematic Changes During Landing Tasks: A Systematic Review. *Int J Exerc Sci*, 12(1), 24-33.
- Tsikopoulos, K., Sidiropoulos, K., Kitridis, D., Cain, S. M., Metaxiotis, D., & Ali, A. (2019). Do External Supports Improve Dynamic Balance in Patients with Chronic Ankle Instability? A Network Meta-analysis. *Clin Orthop Relat Res*. doi:10.1097/CORR.0000000000000946
- Valderrabano, V., Hintermann, B., Horisberger, M., & Fung, T. S. (2006). Ligamentous posttraumatic ankle osteoarthritis. *Am J Sports Med*, 34(4), 612-620. doi:10.1177/0363546505281813
- Valderrabano, V., Horisberger, M., Russell, I., Dougall, H., & Hintermann, B. (2009). Etiology of ankle osteoarthritis. *Clin Orthop Relat Res*, 467(7), 1800-1806. doi:10.1007/s11999-008-0543-6
- Vallandingham, R. A., Gaven, S. L., & Powden, C. J. (2019). Changes in Dorsiflexion and Dynamic Postural Control After Mobilizations in Individuals With Chronic Ankle Instability: A Systematic Review and Meta-Analysis. *J Athl Train*, 54(4), 403-417. doi:10.4085/1062-6050-380-17

- von Tscharner, V. (2000). Intensity analysis in time-frequency space of surface myoelectric signals by wavelets of specified resolution. *J Electromyogr Kinesiol*, 10(6), 433-445.
- von Tscharner, V., & Valderrabano, V. (2010). Classification of multi muscle activation patterns of osteoarthritis patients during level walking. *J Electromyogr Kinesiol*, 20(4), 676-683. doi:10.1016/j.jelekin.2009.11.005
- Wakeling, J. M., & Syme, D. A. (2002). Wave properties of action potentials from fast and slow motor units of rats. *Muscle Nerve*, 26(5), 659-668. doi:10.1002/mus.10263
- Wakeling, J. M., Uehli, K., & Rozitis, A. I. (2006). Muscle fibre recruitment can respond to the mechanics of the muscle contraction. *J R Soc Interface*, 3(9), 533-544. doi:10.1098/rsif.2006.0113
- Wang, X., Ma, Y., Hou, B. Y., & Lam, W. K. (2017). Influence of Gait Speeds on Contact Forces of Lower Limbs. *J Healthc Eng*, 2017, 6375976. doi:10.1155/2017/6375976
- Waterman, B. R., Owens, B. D., Davey, S., Zacchilli, M. A., & Belmont, P. J., Jr. (2010). The epidemiology of ankle sprains in the United States. *J Bone Joint Surg Am*, 92(13), 2279-2284. doi:10.2106/JBJS.I.01537
- Wikstrom, E. A., Hubbard-Turner, T., & McKeon, P. O. (2013). Understanding and treating lateral ankle sprains and their consequences: a constraints-based approach. *Sports Med*, 43(6), 385-393. doi:10.1007/s40279-013-0043-z
- Wikstrom, E. A., Tillman, M. D., Chmielewski, T. L., Cauraugh, J. H., Naugle, K. E., & Borsa, P. A. (2012). Discriminating between copers and people with chronic ankle instability. *J Athl Train*, 47(2), 136-142. doi:10.4085/1062-6050-47.2.136
- Willems, T., Witvrouw, E., Verstuyft, J., Vaes, P., & De Clercq, D. (2002). Proprioception and Muscle Strength in Subjects With a History of Ankle Sprains and Chronic Instability. *J Athl Train*, 37(4), 487-493.
- Wisthoff, B., Matheny, S., Struminger, A., Gustavsen, G., Glutting, J., Swanik, C., & Kaminski, T. W. (2019). Ankle Strength Deficits in a Cohort of College Athletes With Chronic Ankle Instability. *J Sport Rehabil*, 28(7), 752-757. doi:10.1123/jsr.2018-0092

- Wright, C. J., Arnold, B. L., & Ross, S. E. (2016). Altered Kinematics and Time to Stabilization During Drop-Jump Landings in Individuals With or Without Functional Ankle Instability. *J Athl Train*, 51(1), 5-15. doi:10.4085/1062-6050-51.2.10
- Wright, I. C., Neptune, R. R., van den Bogert, A. J., & Nigg, B. M. (2000). The influence of foot positioning on ankle sprains. *J Biomech*, 33(5), 513-519. doi:10.1016/s0021-9290(99)00218-3
- Yoon, J. Y., Hwang, Y. I., An, D. H., & Oh, J. S. (2014). Changes in kinetic, kinematic, and temporal parameters of walking in people with limited ankle dorsiflexion: pre-post application of modified mobilization with movement using talus glide taping. *J Manipulative Physiol Ther*, 37(5), 320-325. doi:10.1016/j.jmpt.2014.01.007